HHS Public Access

Author manuscript

Nat Neurosci. Author manuscript; available in PMC 2021 October 01.

Published in final edited form as:

Nat Neurosci. 2021 April ; 24(4): 516–528. doi:10.1038/s41593-020-00784-3.

Medial Preoptic Area Antagonistically Mediates Stress-induced Anxiety and Parental Behavior

Guang-Wei Zhang[1], **Li Shen**[1], **Can Tao**[1], **A-Hyun Jung**[1,3], **Bo Peng**[1,3], **Zhong Li**[1], **Li I. Zhang**[1,2,*], **Huizhong Whit Tao**[1,2,*]

[1]Zilkha Neurogenetic Institute, Keck School of Medicine, University of Southern California, Los Angeles, CA 90033, USA

[2]Department of Physiology and Neuroscience, Keck School of Medicine, University of Southern California, Los Angeles, CA 90033, USA

[3]Graduate Program in Neuroscience, University of Southern California, Los Angeles, CA 90089, USA.

Abstract

Anxiety is a negative emotional state that is overly displayed in anxiety disorders and depression. Although anxiety is known to be controlled by distributed brain networks, key components for its initiation, maintenance and coordination with behavioral state remain poorly understood. Here, we report that anxiogenic stressors elicit acute and prolonged responses in glutamatergic neurons of mouse medial preoptic area (mPOA). These neurons encode extremely negative valence, and mediate induction and expression of anxiety-like behaviors. Conversely, mPOA GABAergic neurons encode positive valence and produce anxiolytic effects. Such opposing roles are mediated by their competing local interactions and long-range projections to the periaqueductal gray. The two neuronal populations antagonistically regulate anxiety-like and parental behaviors: anxiety is reduced while parenting is enhanced and *vice versa*. Thus, by evaluating negative and positive valences through distinct but interacting circuits, mPOA coordinates emotional state and social behavior.

Anxiety is a state of apprehension associated with heightened arousal and vigilance[1-3]. Anxiety after exposure to stress is an adaptive response, as the anxious state helps the animal maintain caution and cope better with future threats. However, anxiety can become

*Correspondence should be addressed to: L.I.Z. (liizhang@usc.edu) or H.W.T. (htao@usc.edu).

Author Contributions

G.Z. performed behavioral and photometry experiments and data analysis. L.S. performed optrode recording experiments. A.J. contributed to immunohistochemistry experiments and image analysis. C.T. and B.P. performed slice recording experiments. Z.L. helped with the photometry experiments. L.I.Z. and H.W.T supervised the project. H.W.T, G.Z. and L.I.Z. wrote the manuscript.

Reporting Summary

Further information on research design is available in the “Nature Research Reporting Summary” linked to this article.

Code availability

Python code for animal detection is available on https://github.com/GuangWei-Zhang/TraCon-Toolbox. Custom pupil size detection Python code and custom Matlab code for fiber photometry or electrophysiological data analysis will be provided upon request to the corresponding authors.

Competing Interests Statement

The authors declare no competing interests.

maladaptive in conditions such as the post-traumatic stress disorder (PTSD) and major depression, with subjects exhibiting excessive or constant apprehension[2,4,5]. Due to the increasing pressure of life and work in modern society, anxiety disorders are becoming more prevalent and represent a major societal challenge. To improve existing or develop new treatment strategies for anxiety disorders, a thorough understanding of neural circuits governing this emotional state is necessary.

It has been proposed that anxiety is controlled by a large network of distributed brain structures[1,6]. Recent studies have mostly been focused on input and output projections of the amygdala and the bed nucleus of the stria terminalis (BNST). Using optogenetic approaches to manipulate neural activity, it has been shown that both the amygdala and BNST play important roles in acutely controlling anxiety-like behaviors[7-9]. In addition, an extra-amygdala circuit, which goes from the ventral hippocampus (vHPC) to the lateral septum (LS) and then the anterior hypothalamus, contributes to the induction and persistence of a stress-induced anxiogenic state through modulating activity in the paraventricular nucleus of hypothalamus (PVN)[10]. Furthermore, the medial prefrontal cortex (mPFC) interacts with both the vHPC and amygdala[11-13] and may modulate anxiety state based on animals' previous experiences or internal needs[1]. Despite these previous studies, key structures involved in the large anxiety network, especially those critical for the induction and maintenance of anxiety-related phenotypes under different environmental and social contexts, need to be further explored. In addition, circuits through which anxiety state is coordinated with the ongoing behavior remain uncertain.

In the present study, we took a strategy of searching for brain structures that exhibit both acute and prolonged responses to anxiogenic stressors. Considering a close link between anxiety state and prior exposure to noxious stimuli[10,14], brain structures encoding negative valence may be intimately involved in converting the emotional valence to the expression of anxiety-like phenotypes. Here, by exploiting acute stress-induced anxiety paradigms, we identified a structure previously unrecognized in anxiety-related circuits, the medial preoptic area (mPOA). It is a sex-dimorphic structure[15,16] and subsets of its GABAergic neurons have been implicated in parental behavior[17-19] and social preference[20]. We found that glutamatergic neurons in mPOA encode extremely negative valence and mediate anxiety-like behaviors induced by both physical and social stressors. In contrast, GABAergic neurons in mPOA encode positive valence and produce anxiolytic effects. These two neuronal populations also act opposingly in regulating parental behavior. Our results suggest that by evaluating negative and positive valences with distinct but interacting circuits, mPOA functions as a critical center for regulating anxiety-like behaviors and antagonistically coordinating the anxiety state and rewarding social behavior.

Results

Activation of mPOA glutamatergic neurons by physical stressors

We subjected mice to several different types of noxious stimuli, such as forced swimming, heat plate, and electric shocks (Fig. 1a, see Methods), and tested anxiogenic effects of these stimuli one hour after by using two standard behavioral assays: the open field test (OFT) and elevated plus maze (EPM) test[7,8,10,21]. In OFT (Fig. 1b), mice exposed to either one of the

stressors spent less time in the center zone than the respective control animals experiencing the same experimental contexts within a 20-min test session (Fig. 1c, see control condition in Extended Data Fig. 1a,b). In EPM (Fig. 1d), the open-arm time within a 5-min test session was reduced in mice exposed to stressors compared with control animals (Fig. 1e). These behavioral results suggest an elevated anxiety state after exposure to stressors, consistent with previous studies[7,14,21,22].

Next, we examined which brain areas exhibited acute or prolonged activity after stress exposure by using c-fos staining (Extended Data Fig. 1c-d, see Methods). Animals were sacrificed 3 hrs after stress exposure, as it takes about 2-3 hrs for the c-fos protein expression to peak after neuronal activation[23]. A higher level of c-fos expression was observed in mPOA than control animals after exposure to electric shocks (Fig. 1f,g). Increased staining was also observed in the amygdala (Amg), BNST and periaqueductal gray (PAG) (Fig. 1f), the three structures that have been previously implicated in anxiety[1,3]. Similarly, increased c-fos expression was observed in mPOA after exposure to other types of stressors (Fig. 1h). About 80% of activated mPOA neurons were glutamatergic, as shown by the colocalization of c-fos and Vglut2 signals (Fig. 1i,j), and about 60% of glutamatergic neurons in mPOA were detected to be activated after exposure to electric shocks (Fig. 1j). Neurons activated by different stressors appeared to distribute randomly within mPOA (Extended Data Fig. 1e), considering the endogenous expression pattern of Vglut2 (Extended Data Fig. 1f,g).

We next examined directly whether glutamatergic neurons in mPOA could be acutely activated by the physical stressors. By injecting adeno-associated virus (AAV) encoding Cre-dependent GCaMP6s in mPOA of Vglut2-Cre mice[24], we monitored Ca^{2+} signals in freely moving animals with photometry[25] (Fig. 1k). All testing stressors induced large increases of Ca^{2+} (Fig. 1k,m, Extended Data Fig. 2a-d), confirming that mPOA glutamatergic neurons can be acutely activated by various types of stressors. Control experiments showed no or minimum motion artifacts in our experimental conditions (Extended Data Fig. 2e-k). In addition, we noticed that the baseline fluorescence preceding the onset of shocks gradually increased over repeated applications (Fig. 1l, Extended Data Fig. 3a), suggesting that the spontaneous firing activity might be increased. As photometry data lacked single-cell resolutions, to further examine the spontaneous activity of mPOA glutamatergic neurons, we recorded from optogenetically identified glutamatergic neurons (onset latency of light-evoked spikes: 2.8 ± 0.8 ms, mean ± s.d.) using optrodes in Vglut2::ChR2 mice (Fig. 1n, Extended Data Fig. 3b). Indeed, the spontaneous firing rate of these neurons increased for hours after the cessation of electric shocks but remained stably low in control animals (Fig. 1o, Extended Data Fig. 3c). Overall, the increase persisted for about 4 hours (Extended Data Fig. 3d), consistent with the behavioral result of an elevated anxiety state for about 4 hours after stress exposure (Extended Data Fig. 3e). Furthermore, nearly all recorded mPOA glutamatergic neurons responded acutely to multiple types of stressors (Extended Data Fig. 3f,g). For non-phototagged neurons (presumably GABAergic neurons), 54% showed no acute response to stress, 23% were activated, and 23% were suppressed (Extended Data Fig. 3h). The spontaneous firing rate of these neurons was essentially unchanged after stress exposure (Extended Data Fig. 3i). Together, our results suggest that mPOA glutamatergic neurons acutely respond to a variety of stressor stimuli, and their baseline activity increases for a considerably long period of time after exposure to stress.

Activation of glutamatergic mPOA neurons induces negative valence and anxiety-like behaviors

To test whether mPOA is involved in stress-induced anxiety, we optogenetically stimulated mPOA glutamatergic neurons by virally expressing ChR2 in Vglut2-Cre mice (Fig. 2a, Extended Data Fig. 4a,b). We first confirmed the high efficacy of ChR2 activation using slice whole-cell recordings (Fig. 2b). By injecting currents (square or ramp) into the recorded cells, we found that mPOA glutamatergic neurons could be driven to fire action potentials at frequencies up to ~15Hz (Fig. 2c). Since these neurons could be activated by aversive stimuli, we tested whether their activity encoded negative valence by using a two-chamber real-time place preference test (PPT)[8,26,27]. LED stimulation was applied whenever the animal stayed in the designated stimulation (LED-on) chamber (Fig. 2d). The ChR2-expressing animals spent much less time in the LED-on chamber than GFP control animals, with the latter spending about equal amounts of time in randomly assigned LED-on and LED-off chambers (Fig. 2e, and Supplementary Video 1-2). No obvious sex difference was observed (Fig. 2e). Thus, activation of mPOA glutamatergic neurons is aversive. In addition, 24 hours after the exposure to LED stimulation, animals still exhibited avoidance from the LED-on chamber even though no LED light was applied (Extended Data Fig. 5a,b), indicating that activation of the mPOA neurons can drive conditioned place avoidance (CPA).

We further examined whether increasing mPOA glutamatergic neuron activity could acutely enhance anxiety-like behaviors (Fig. 2f). Compared with GFP control animals, activation with continuous LED light pulses (at 10 Hz) reduced the center time in OFT (Fig. 2g) and the open-arm time in EPM (Fig. 2f,h), and similar effects were observed in both sexes. These effects increased with increasing stimulation frequencies (Extended Data Fig. 5c,d). In the meantime, the optogenetic stimulation induced pupil dilation (Fig. 2i,j) and increased locomotion (Fig. 2k) without any location specificity (Extended Data Fig. 5e-h). These behavioral patterns are suggestive of high arousal levels[28], consistent with the notion that anxiety is associated with elevated arousal and vigilance[1-3].

We also applied chemogenetics for activating mPOA glutamatergic neurons, by expressing a Cre-dependent excitatory DREADD receptor, hM3Dq (Extended Data Fig. 4c). In slice recordings, we confirmed that application of the DREADD agonist, Clozapine-N-oxide (CNO), induced depolarization of the membrane potential (and increases of firing rate) in hM3Dq-expressing mPOA neurons (Extended Data Fig. 5i-k). In freely moving animals, chemogenetic activation by CNO administration reduced the center time in OFT and open-arm time in EPM as compared with mCherry control animals (Extended Data Fig. 5l,m). In addition, optogenetic stimulation of mPOA glutamatergic neurons for 5 min resulted in elevated anxiety-like behaviors one hour after the stimulation (Extended Data Fig. 5n-p), suggesting that activity of these neurons promotes the initiation of an anxiety state.

Strong activation of mPOA glutamatergic neurons (at 15Hz) apparently caused extremely aversive emotion. In conflict tests where a physical stressor (electric shocks, heat plate or cold water) was present in the LED-off side of a test box, ChR2-expressing animals avoided the LED-on side (Extended Data Fig. 6a-c, and Supplementary Video 3-4). In addition, in a single-chamber box, the strong activation of mPOA glutamatergic neurons greatly increased

the frequency of rearing and even more dramatically triggered animal jumping (Extended Data Fig. 6d-g). It also suppressed food intake in hungry mice (Extended Data Fig. 6h). Similar effects were observed in animals with mPOA glutamatergic neurons chemogenetically activated (Extended Data Fig. 6i-k). These behavioral results suggest that mPOA glutamatergic neurons can encode strongly negative valence.

Suppression of mPOA glutamatergic neurons reduces anxiety-like behaviors

To further test whether mPOA glutamatergic neurons mediate stress-induced anxiety, we silenced these neurons by expressing a Cre-dependent inhibitory DREADD receptor, hM4Di (Extended Data Fig. 4d). Slice whole-cell recording confirmed that application of CNO could prevent spiking of hM4Di-expressing mPOA neurons (Fig. 3a,b). In OFT, hM4Di-expressing animals with CNO injected at 40 min after stress exposure spent more time in the center zone than mCherry control animals and saline-injected hM4Di-expressing animals (Fig. 3c,d). Similarly, the open-arm time in EPM was also largely increased in CNO-injected hM4Di animals (Fig. 3e,f). These results indicate that silencing mPOA glutamatergic neurons suppresses stressor-induced anxiety-like behaviors.

In a parallel set of experiments, we optogenetically silenced mPOA glutamatergic neurons by expressing Cre-dependent ArchT (Extended Data Fig. 4e). Slice whole-cell recording confirmed that green LED light induced a membrane hyperpolarization in ArchT-expressing mPOA neurons, which prevented their spiking (Fig. 3g,h). Optogenetic silencing of mPOA glutamatergic neurons resulted in a weak place preference (Extended Data Fig. 6l-n). We next tested the optogenetic silencing in OFT one hour after exposure to electric shocks (Fig. 3i), with LED-off and LED-on blocks (3 min per block) interleaved during the test. For LED-on blocks, the ArchT-expressing animals exhibited significantly more center time than GFP control animals, whereas in LED-off blocks these two groups of animals did not show a significant difference (Fig. 3j). In EPM, the optogenetic silencing increased the open-arm time compared with GFP animals (Fig. 3k,l).

Together, the results of above activation and inactivation experiments suggest that mPOA glutamatergic neurons mediate the expression of physical stress-induced anxiety-like behaviors. We further tested the role of these neurons in the induction of anxiety-like behaviors by optogenetically silencing them only during exposure to shocks. This resulted in increases in center-time and open-arm time compared with GFP animals (Extended Data Fig. 6o,p), indicating that the acute responses of mPOA glutamatergic neurons to stressors may be required for the induction of anxiety-like behaviors.

mPOA antagonistically regulates social stress-induced anxiety and parental behavior

Previously, mPOA has been implicated in social behaviors such as parenting and social preference[18-20]. We wondered whether this structure could also play a role in socially induced anxiety. Following a previous study[19], we introduced a younger male mouse (intruder) or a foreign pup into the home cage of a resident virgin male for 15 min. This resulted in elevated anxiety-like behaviors in the resident, as shown by OFT and EPM tests performed at 40 min after the exposure (Extended Data Fig. 7a,b). Thus, male intruders and foreign pups are social stressors to virgin males. Using fiber photometry, we imaged Ca^{2+}

activity of mPOA glutamatergic neurons during social interactions (Fig. 4a). We found that in virgin male mice, bouts of interactions with an intruder or a pup elicited large increases of Ca^{2+} activity in mPOA glutamatergic neurons (Fig. 4b-d). In contrast, no increase was observed when a virgin male interacted with a female intruder or when a virgin female interacted with a foreign pup (Fig. 4e-f). These results indicate that mPOA glutamatergic neurons can be activated by social stressors but not by social rewards.

Optogenetically silencing mPOA glutamatergic neurons during OFT and EPM tests performed after exposure to social stress reduced anxiety-like behaviors (Fig. 4g,h), suggesting that these neurons also mediate the expression of social stress-induced anxiety-like behaviors. Silencing these neurons during the 15-min exposure to a male intruder greatly reduced chances of the resident male fighting against the intruder (Fig. 4i), indicating reduced inter-male aggression[19], which is possibly attributed to reduced anxiety[29]. In addition, the treatment impaired the expression of anxiety-like behaviors after the intruder exposure (Fig. 4j), suggesting that activity of mPOA glutamatergic neurons is also required for the induction of social anxiety.

We also tested anxiety-like behaviors induced by pup exposure. Optogenetic silencing of mPOA glutamatergic neurons after the exposure reduced anxiety-like behaviors (Fig. 4k,l). During the pup exposure, the virgin male displayed pup-directed aggression (Fig. 4m), as reported previously[19]. Photo-inactivation of mPOA glutamatergic neurons whenever the male started to explore the pup largely suppressed pup attack (Fig. 4m) and increased duration of pup grooming (Extended Data Fig. 7c), indicating reduced pup-directed aggression and enhanced parenting, respectively. Furthermore, the photoinactivation during pup exposure greatly reduced the later expression of anxiety-like behaviors (Fig. 4n), again indicating that acute responses of mPOA glutamatergic neurons to social stressors are required for the induction of anxiety-like behaviors.

In contrast to virgin males, in virgin females exposure to a foreign pup did not lead to elevated anxiety-like behaviors (Extended Data Fig. 7d), consistent with the photometry data that mPOA glutamatergic neurons in virgin females were not activated by interacting with pups (Fig. 4f). Nonetheless, optogenetic inactivation of mPOA glutamatergic neurons in virgin females reduced anxiety-like behaviors (Fig. 4o,p) regardless of pup exposure (Extended Data Fig. 7e). During the pup exposure, the inactivation greatly increased chances of pup retrieval (Fig. 4q) and prolonged duration of pup grooming (Fig. 4r), indicating enhanced parenting. Together, these results support the notion that when anxiety state is suppressed, social aggression is reduced while parental behavior is promoted (in both sexes). Therefore, mPOA-mediated emotional state is tightly linked to social behaviors.

It appears that silencing mPOA glutamatergic neurons can reduce anxiety-like behaviors even in animals without exposure to stressors (Extended Data Fig. 7e,f). We further examined basal-level anxiety-like behaviors using additional assays. Chemogenetic silencing of mPOA glutamatergic neurons reduced the time in shelter in an open field test (Extended Data Fig. 7g) as well as the time in the lit side in a dark-light box test[30] (Extended Data Fig. 7h). These results further support the notion that mPOA glutamatergic neurons regulate basal-level anxiety-like behaviors as well.

The mPOA to PAG pathway mediates anxiety-like behaviors

We next explored downstream targets of mPOA. Tracing axons from GFP-labelled mPOA glutamatergic neurons, we found that these cells projected strongly to PAG, lateral hypothalamic area (LHA) and superior mammillary body (SuM) (Fig. 5a, and Extended Data Fig. 8a). By photo-stimulating ChR2-expressing mPOA glutamatergic axons (at 15 Hz) in these target areas, we observed anxiety-like behaviors such as jumping and aversion phenotypes when the mPOA to PAG (but not to LHA or SuM) pathway was activated (Extended Data Fig. 8b-d). We thus focused on PAG. Injection of AAVretro-Cre in PAG of Cre-dependent tdTomato reporter (Ai14) mice resulted in retrograde labeling of neurons in mPOA (Fig. 5b). To further confirm the functional connectivity, we expressed ChR2 in mPOA glutamatergic neurons and made slice whole-cell recordings from PAG neurons (Fig. 5c). With TTX and 4AP present in the bath solution, we observed LED-evoked monosynaptic excitatory postsynaptic currents (EPSCs) in recorded PAG neurons (Fig. 5d), confirming that PAG neurons receive direct excitatory input from mPOA.

In freely moving mice, we specifically activated mPOA glutamatergic terminals in PAG by implanting optic fibers above PAG (Fig. 5e). LED stimulation reduced the time in the LED-on chamber in PPT (Fig. 5f), consistent with the notion that these axons relay signals of negative valence. The stimulation also increased baseline locomotion in an open arena (Fig. 5g), as well as reduced the center time in OFT (Fig. 5h) and the open-arm time in EPM (Fig. 5i), similar to stimulating the mPOA neurons *per se*. To further demonstrate the involvement of the mPOA→PAG pathway, we expressed ChR2 in PAG-projecting mPOA neurons by injecting AAVretro-Cre in PAG and AAV encoding Cre-dependent ChR2 in mPOA (Fig. 5j, and Extended Data Fig. 8e). We also expressed ChR2 in mPOA-recipient PAG neurons by injecting AAV1-Cre in mPOA and AAV encoding Cre-dependent ChR2 in PAG[31,32] (Fig. 5o, and Extended Data Fig. 8f). Optogenetic stimulation of PAG-projecting mPOA neurons or mPOA-recipient PAG neurons produced effects similar to stimulating mPOA→PAG axons: place avoidance (Fig. 5k,p), increased locomotion (Fig. 5l,q), reduced center time in OFT (Fig. 5m,r) and reduced open-arm time in EPM (Fig. 5n,s). Additionally, we expressed hM4Di in mPOA glutamatergic neurons and injected CNO locally[33] in PAG to specifically silence mPOA→PAG axon terminals (Fig. 5t). This again reduced anxiety-like behaviors after exposure to electric shocks (Fig. 5u,v). Together, these results suggest that the glutamatergic mPOA→PAG pathway can largely account for the mPOA's role in regulating anxiety.

We further examined whether the glutamatergic mPOA→VTA pathway could be involved in the anxiety regulation. The glutamatergic mPOA→VTA axons were relatively sparse (Extended Data Fig. 9a). Activation of these axons induced weak aversion phenotypes but did not affect anxiety-related behaviors (Extended Data Fig. 9b-d). Injections of CTb of different colors in PAG and VTA respectively revealed that PAG- and VTA-projecting mPOA neurons were essentially separate neuronal populations (Extended Data Fig. 9e-g). Consistently, retrograde labeling of PAG-projecting mPOA neurons with AAVretro resulted in extremely sparse axon collaterals in VTA (Extended Data Fig. 9h,i). These data indicate that our optogenetic stimulation of mPOA→PAG axon terminals unlikely affects

mPOA→VTA axons and that mPOA glutamatergic neurons enhance anxiety-like behaviors primarily through their projection to PAG.

GABAergic mPOA neurons play an opposite role in regulating anxiety and parental behavior

About half of mPOA neurons are GABAergic[34]. Using Vgat-Cre mice, we next examined whether the GABAergic neurons also played a role in regulating anxiety-like behaviors. Stimulating GABAergic mPOA neurons (Fig. 6a) produced strong place preference (i.e. positive valence) in both males and females (Fig. 6b), reversibly increased the center time in OFT (Fig. 6c) as well as increased the open-arm time in EPM (Fig. 6d). Activation of these neurons also enhanced parental behaviors in virgin females (Fig. 6e,f) while reduced pup-directed aggression in virgin males (Fig. 6g). No effect was observed in GFP control mice (Extended Data Fig. 10a-e). Thus, GABAergic and glutamatergic mPOA neurons play opposite roles in regulating both anxiety-like and parental behaviors.

We next explored intra-mPOA connectivity by specifically expressing ChR2 in mPOA GABAergic neurons in Vgat-Cre::Ai14 mice. As Vglut2+ and Vgat+ neurons are separate populations and together cover almost all the neurons in mPOA[34], we were able to record selectively from glutamatergic neurons in slice preparations while optically stimulating GABAergic neurons (Fig. 6h). Strong light-evoked monosynaptic inhibitory postsynaptic currents (IPSCs) were observed (Fig. 6i), indicating that GABAergic neurons can suppress glutamatergic neurons locally.

Slice recording revealed that GABAergic neurons provided direct inhibitory input to PAG neurons (Fig. 6j,k). We then tested the functional impact of this long-range inhibitory projection. Photo-stimulation of GABAergic mPOA→PAG terminals (Extended Data Fig. 10f) produced place preference (Fig. 6l,m), reduced anxiety-like behaviors (Fig. 6n,o), enhanced parental behavior in females (Fig. 6p) and reduced pup-directed aggression in males (Fig. 6q). Therefore, mPOA GABAergic neurons regulate both anxiety-like and parental behaviors in an antagonistic manner to the glutamatergic neurons not only by locally inhibiting the glutamatergic neurons but also by sending a competing (i.e. inhibitory) projection to PAG.

Inputs to mPOA glutamatergic neurons

What are input sources to mPOA glutamatergic neurons? To address this question, we applied cell-type-specific retrograde tracing of monosynaptic inputs using pseudotyped rabies virus[35] (Fig. 7a). Retrogradely labeled cells were observed in a number of regions, in particular LS, BNST and PVN (Fig. 7b,c). The latter structures have all been implicated previously in anxiety or stress responses[1,3,36-39]. These identified input structures are in general consistent with previous anatomical results[40] and suggest that the mPOA neurons may integration information of aversive events from multiple sources.

Discussion

In the present study, we found that mPOA glutamatergic neurons are activated by exposure to anxiogenic stressors and that their baseline firing rates are increased for a long period of

time after the exposure. Cell-type specific examination revealed opposite roles of mPOA glutamatergic and GABAergic neurons in regulating anxiety-like behaviors: the glutamatergic neurons enhance anxiety-like behaviors and mediate stress-induced anxiety states, whereas the GABAergic neurons suppress anxiety-like behaviors. The GABAergic neurons antagonize the effects of the glutamatergic neurons not only by locally inhibiting the latter but also by sending a parallel but competing projection to the common target, PAG. In addition, these two neuronal populations both antagonistically coordinate anxiety-like and parental behaviors: enhancing anxiety-like while reducing parental behaviors, and *vice versa*. These results, for the first time to our knowledge, implicate mPOA in the anxiety-related network. In particular, mPOA may play an important role in coordinating emotional state and social behavior.

The mPOA glutamatergic neurons generally modulate anxiety states

Although mPOA has been previously implicated in a variety of fundamental functions, including sleep, hunting, mating and parenting[15,18-20,41,42], these functional roles have mostly been attributed to its GABAergic populations expressing differential molecular markers besides GABA[34]. The functional role of its glutamatergic population has yet remained unclear. Here, our results indicate that mPOA serves as a critical center to regulate anxiety states through its glutamatergic neurons. Activating these cells can directly trigger anxiety-like behaviors, while silencing them alleviates the expression of anxiety-like behaviors after exposure to a variety of physical and social stressors. While these effects were observed in both sexes in our experimental conditions, we do not exclude any possibilities of sex differences (e.g. different activation thresholds for the induction of anxiety-like behaviors). The baseline firing rates of these neurons are increased for a relatively long period of time after stress exposure, which accounts for the persistence of the induced anxiety state. In addition, suppressing the baseline activity of these neurons is sufficient to reduce basal-level anxiety-like behaviors. Furthermore, their activity during the exposure to stressors is required for and promotes the induction of an anxiety state. Together, our results demonstrate that mPOA glutamatergic neurons regulate the induction, expression and maintenance of anxiety states in general.

Our additional experiments indicate that mPOA glutamatergic neurons are not involved in hunting-like behaviors or thermal regulation (Extended Data Fig. 10g-i), functions that have been reported for a different molecularly defined cell group ($CaMKII\alpha^+$) in mPOA and glutamatergic neurons in a spatially close nucleus (vLPO) of the preoptic area, respectively[41,43]. This excludes the possibility that the elevated anxiety state resulting from the activation of mPOA glutamatergic neurons is due to a side effect of changes in body temperature. On the other hand, the elevated anxiety state is in line with the observed increase in wakefulness[42], as anxiety disorders are often accompanied by sleep problems[44].

The mPOA glutamatergic neurons likely receive information of aversive cues/events from multiple sources including LS, BNST and PVN (Fig. 7). Neurons of these structures have been shown to respond to aversive stimuli[8,10,36]. Therefore, the mPOA glutamatergic neurons may be able to integrate multiple types of information to potently regulate anxiety states under diverse sensory and social contexts. Multiple mechanisms may underlie the

enhanced baseline activity of these neurons after stress exposure: increases in the synaptic strength of their inputs, in the intrinsic excitability of these neurons *per se*, and/or in the spiking activity of any of their input structures. In other words, “stress memory” may be stored locally within mPOA or remotely in its upstream structures.

The mPOA glutamatergic neurons can encode extremely negative valence

Regulation of negative emotions, including fear and anxiety, depends on the processing of negative valence[1,3,45]. Compared to previously studied structures such as BNST[8] and PVN[36], activation of mPOA glutamatergic neurons appears to result in an extremely strong negative emotion. Noticeably, in PPT, the percentage time spent in the photo-stimulation chamber (Fig. 2e) is less than when other structures are activated[8,36], and animals exhibit frequent rearing and jumping behaviors when put in an inescapable context (Extended Data Fig. 6d-g). More strikingly, in conflict tests animals prefer to stay in places where physical harms could be inflicted rather than those only associated with the photo-stimulation (Extended Data Fig. 6a-c). These results provide strong evidence that activity of mPOA glutamatergic neurons can encode extremely negative valence, and thus may lead to a severely anxious state. This property of mPOA glutamatergic neurons suggests that they might be a unique therapeutic target for treating severe anxiety disorders.

An opposite role of mPOA GABAergic neurons

Opposite to the glutamatergic neurons, our results demonstrate that the mPOA GABAergic neurons as a whole population encode positive valence and promote parental behavior. This is consistent with observations in previous studies on molecularly identified subpopulations of GABAergic neurons in mPOA[15,18-20,34]. For example, both Gal^+ and $Esr1^+$ mPOA neurons promote rewarding phenotypes and parental behavior[18,19], and Nts^+ mPOA neurons encode attractive male cues and promote social approach in females[20]. Notably, by comparing glutamatergic and GABAergic neurons, our current study reveals that the rewarding phenotype (i.e. place preference) induced by activating the GABAergic neurons is much stronger than silencing the glutamatergic neurons themselves (compare Fig. 6b and Extended Data Fig. 6l-n). This further indicates that activity of the glutamatergic neurons cannot encode a full spectrum of valence values and that positive valence is mainly coded by the GABAergic neurons. Besides valence coding, our study further reveals that activity of the GABAergic neurons is strongly anxiolytic, as activation of these neurons greatly suppresses anxiety-like behaviors and social aggression. It is likely that rewarding social cues, by activating mPOA GABAergic neurons[19,20], can directly generate anxiolytic effects. Our results suggest that targeting mPOA GABAergic neurons might be another powerful therapeutic strategy for anxiety disorders.

Antagonistic control of anxiety state and parenting by mPOA neurons

Previously, an antagonistic relationship between anxiety- and parenting-related behaviors has been documented: enhanced anxiety is known to suppress parental behavior[46], while reduced anxiety has been observed in postpartum animals that show elevated parental behavior[47,48]. In the present study, the finding that manipulating mPOA neurons affects both parenting and anxiety levels demonstrates that mPOA plays a critical role in coordinating the anxiety state and parental behavior. Such coordination is likely achieved through competitive

interactions between the glutamatergic and GABAergic neurons: the GABAergic neurons locally inhibit the glutamatergic neurons, and compete with the latter through their long-range inhibitory projections to the common target, PAG, which has been implicated in providing motor commands for parental behavior[49]. While the glutamate neurons promote an anxiety state and the GABA neurons promote parental behaviors, coordinating the relative activity in the two populations determines which type of behavior is expressed (Extended Data Fig. 10o). It is also possible that the glutamatergic neurons suppress parental behaviors in an indirect manner, since promoting anxiety can non-specifically suppress affiliative behavior. Additional retrograde labeling experiments suggest that about two-thirds of PAG-projecting mPOA neurons are glutamatergic while about one third is GABAergic (Extended Data Fig. 10j-n). This provides an explanation for the result that activating PAG-projecting mPOA neurons as a population produces a similar but weaker effect than activating mPOA glutamatergic axons in PAG (compare Fig. 5f and Fig. 5k).

Functional relationship between mPOA and BNST

A spatially proximate nucleus, BNST, has been previously implicated in physical stress-related anxiety[8]. In particular, glutamatergic and GABAergic neurons in the ventral BNST (vBNST) have been shown to encode opposing motivational states and produce anxiogenic and anxiolytic behavioral phenotypes, respectively[8,39]. mPOA and vBNST can be clearly distinguished based on their differences in anatomical characteristics (e.g. input/output organization)[40,50] as well as distributions of molecularly identified cell types[34,40] (also see Extended Date Fig. 1f,g). Considering that mPOA receives axonal projections unidirectionally from BNST (Extended Data Fig. 4a), it is possible that the two structures can play some similar functional roles in regulating physical stress-induced anxiety. However, as they have different input/output connectivity patterns, the two structures may also exhibit distinct functional roles under different sensory and behavioral contexts. We speculate that mPOA may play a more unique role in mediating socially induced anxiety states.

In summary, we have identified mPOA as a previously unrecognized structure to control anxiety state and to mediate the induction and expression of stress-induced anxiety-like behaviors. We propose that activity of mPOA glutamatergic and GABAergic neurons is highly correlated with the value of negative and positive valences, respectively. The balance between activities of these neurons through competitive interactions may thus allow the expression of the emotional state under different sensory and social contexts with a broad dynamic range.

Methods

Animal experiments were conducted in accordance with the guidelines for the care and use of laboratory animals of US National Institutes of Health (NIH), and under protocols approved by Institutional Animal Care and Use Committee at University of Southern California, and Southern Medical University.

Animals

The Vglut2-*ires*-Cre (Jackson stock No. 016963), Vgat-ires-Cre (Jackson stock No.016962), Ai14 (Cre-dependent tdTomato reporter line, Jackson stock No. 007914), Ai27 (Cre-dependent ChR2 reporter line, Jackson stock No.012567) and Ai75 (Cre-dependent nuclear-localized tdTomato reporter line, Jackson stock No.025106), Dat-*ires*-Cre (Jackson stock No.006660), C57BL/6 mice were obtained from the Jackson Laboratory. Mice were housed at 18-23°C with 40-60% humidity in a 12h light-dark cycle with ad libitum access to food and water. Experiments were performed in adult male and female mice (6-12 weeks old) during the dark cycle. Regarding animal cohorts, in general, a cohort of mice were subjected to a battery of anxiety-like behavioral assays, with at least 72 hr gaps, to reduce the total number of animals used. However, animals in a cohort might not undergo the same number of tests due to changes in animal conditions (e.g. broken optical cannula). Separate groups of mice were used for different control treatments in Fig. 1c. In Fig. 2, separate cohorts were used for the valence test and anxiety-like behavior tests.

Virus

AAV2/1-pEF1a-DIO-hChR2-eYFP (1.82×10^{13} GC/ml, UPenn vector core), AAV1-CAG-FLEX-GFP-WPRE (2×10^{13} GC/ml, UPenn vector core, Addgene 51502), AAVretro-Cre (1.5×10^{14} GC/ml, Vigene)[51], AAV1-CAG-FLEX-ArchT-GFP (4×10^{12} GC/ml, UNC vector core), pAAV-hSyn-DIO-hM3D(Gq)-mCherry (1.3×10^{13} GC/ml, Addgene 44361), pAAV-hSyn-DIO-hM4D(Gi)-mCherry (3×10^{13} GC/ml, Addgene 44362), pAAV-hSyn-DIO-mCherry (4.8×10^{13} GC/ml, Addgene 50459), AAV1-Syn-FLEX-GCamp6s-WPRE-SV4 (Addgene 100845), AAV1-DIO-FLPo-WPRE-hGHpA (1.53×10^{14} GC/ml, Addgene 87306), AAV8-CAG-fDIO-TVA-mCherry (1.1×10^{13} GC/ml, Salk Institute), AAV_{DJ}-CAG-fDIO-oG-WPRE(4.4×10^{13} GC/ml, Salk Institute), EnvA-G-deleted Rabies-GFP (8.13×10^{9} GC/ml, Salk Institute) were used in this study. The volume for each injection was 50 nl.

Surgical procedures

Mice were anesthetized with 1.5-2% isoflurane. A small cut was made on the skin covering the craniotomy position and the muscles were removed. One ~0.25-mm^2 craniotomy window was made for each region. The adeno-associated viruses (AAVs, encoding ChR2, ArchT, hM4D(Gi), hM3D(Gq), GFP, mCherry, GCamp6s) were used depending on the purpose of experiments and strain of mice. A beveled glass micropipette (pulled using MODEL P-97, Sutter Instrument Co., tip diameter: 10-20 μm) was used to deliver the virus. Virus was either delivered by either pressure injection or iontophoresis and the glass micropipette was attached to a microsyringe pump (World Precision Instruments). For pressure injection, 50 nl of the viral solution was injected at a rate of 15 nl/min. For iontophoresis injection, 3 μA current was applied (7 sec on, 7 sec off cycle) for 5 min. After the injection, the pipette was allowed to rest for 5 min before withdrawal. The scalp was then sutured. Following the surgery, 0.1 mg/kg buprenorphine was injected subcutaneously before returning the animals to their home cages. Mice were allowed to recover for at least two weeks before cannula implantation, behavioral test or recording experiments. After each experiment, the brain was sectioned and automatically imaged under a confocal microscope to confirm viral expression. Image tiles were online stitched (FluoView FV1000, Olympus).

For optogenetic manipulations, animals were anesthetized with isoflurane and optic cannula (400 μm, Thorlabs) was stereotaxically implanted into the targeted region depending on the purpose of experiments (mPOA, bilateral implantation, AP +0.9 mm, ML +1.3 mm, DV −4.75 mm, with a 10° angle; PAG, bilateral implantation, AP −4.4, ML +1.5 mm, DV −2.2 mm; vLPO, bilateral implantation, AP +0.9 mm, ML +2 mm, DV −5.2 mm, with a 10° angle; MnPO, unilateral implantation, AP, +1.5mm, ML, +0.2 mm, DV, −4.4mm on a 10° posterior angle; VTA, bilateral implantation, AP, −3.28 mm, ML, 0.4 mm, DV, −4.1 mm). The optic cannula was fixed with dental cement. The mice were allowed to recover for at least one week before the behavior tests. After each experiment, the brain was sectioned and imaged under a confocal microscope to confirm locations of viral expression and the implantation site. For pharmacological manipulations, animals were anesthetized with isoflurane and a drug cannula (RWD Inc., internal diameter: 140 μm) was stereotaxically implanted into target region based on the purpose of experiments.

In vivo optogenetic stimulation

During the 3 days before behavioral tests, animals were attached to optical fibers without LED stimulation for habituation. On the test day, the optic fiber (200 μm core, NA 0.22, Thorlabs) was connected to a blue LED source (480 nm, 0-30 Hz pulses, 5-ms pulse duration, Thorlabs) for stimulation, or a green LED source (530 nm, constant illumination as described in each behavioral test). The LED power measured at the tip of the fiber (connected with optic cannula) is around 3-5mW. The blue light LED stimulation frequency was 10Hz in most experiments, which is within the physiological range of firing rates of the Vglut2 neurons in mPOA. Repeated LED-on and LED-off epochs were applied in Fig. 2j, Fig. 3j and Fig. 6c. In Fig. 2j, data of pupil size were averaged over trials for each animal. In Fig. 3j and Fig. 6c, only one test session was performed in each animal and data for each individual epoch were averaged for all animals.

In vivo chemogenetic manipulation

For DREADD experiments, animals expressing hM4D(Gi) or hM3D(Gq) received either intraperitoneal (IP) injection of clozapine-N-oxide (CNO) (1 mg/kg), or a local infusion of CNO (5 μM, 150 nl) through the implanted cannula to the targeted region.

Fiber photometry recording

To obtain calcium signals, LED light (480nm, Thorlabs) was bandpass filtered (ET470/24M, Chroma), focused by an objective lens (Olympus, Japan), and coupled to an optical fiber (O.D. = 400 μm, NA = 0.48, 1 m long, Doric). The fiber was connected to the implanted optic fiber (400 μm, NA = 0.5, Thorlab) using a ceramic sleeve. The LED power was adjusted to be 0.02 mW at the tip of the optical fiber. At this power, no significant photo bleaching was observed. The fluorescence calcium signal was bandpass filtered (ET525/36M, Chroma) and collected by a photomultiplier tube (H11706-40, Hamamatsu, Japan), then through an amplifier (MODEL SR570, Stanford Research System) and low-pass filtered (30 Hz). The current signal was converted to voltage signal using data acquisition card (PCI-MIO-16E-4, National Instrument) and digitalized at 250Hz. Data were obtained using custom LabVIEW software and off-line analyzed using custom MATLAB software. No movement-related artifact has been detected in our system.

Electrophysiological recording and spike sorting

Multi-channel recording was carried out with a 16-channel silicone probe (A1x16-Poly2-5mm-50s-177-A16, 16 contacts separated by 50 μm, Neuronexus Technologies). Signals were recorded and filtered through a bandpass filter (0.3 - 3 kHz). The nearby four channels of the probe were grouped as tetrodes, and semiautomatic spike sorting was performed by using Offline Sorter (Plexon Inc.). Semi-automated clustering was carried out based on the first three principal components of the spike waveform on each tetrode channel using a T-Dist E-M scan algorithm (scan over a range of 10-30 degree of freedom) and then evaluated with sort quality metrics. Clusters with isolation distance < 20 and L-Ratio > 0.1 were discarded. Spike clusters were classified as single units only if the waveform SNR (Signal to Noise Ratio) exceeded 4 (12 dB) and the inter-spike intervals exceeded 1.2 ms for > 99.5% of the spikes.

Optrode recording

The Vglut2-positive neurons were genetically tagged by crossing Vglut2-Cre mice with Ai27 mice (Cre-dependent ChR2 reporter line). The optrode (A1x16-Poly2-5mm-50s-177-OA16LP, 16 contacts separated by 50 μm, the distance between the tip of the optic fiber and the probes is 200 μm, NA 0.22, Neuronexus Technologies) was connected to a LED light source (480 nm, Thorlabs) with an optic fiber. To identify ChR2+ neurons, 5 or 10 Hz (5-ms pulse duration, 100-ms total duration, controlled via an Arduino microcontroller) LED pulse trains were delivered intermittently, after we finished recording spontaneous activity. To assess whether these units were driven directly by ChR2 or indirectly by synaptic connections, we analyzed the onset latency relative to each light pulse. Only spikes with latency < 4 ms were considered as being directly stimulated in this study. We analyzed the waveform similarity between LED-evoked and spontaneously generated spikes, and correlation coefficient > 0.9 was used as a criterion for determination of the same unit.

Image acquisition

To check the expression of eYFP, GFP or mCherry, or electrode tracks (coated with DiI), the animals were deeply anesthetized using urethane (25%) and transcardially perfused with phosphate-buffered saline (PBS) and paraformaldehyde (4% in PBS). Coronal brain sections (150 μm) were made with a vibratome (Leica Microsystems) and stained with Nissl reagent (Deep red, Invitrogen) for 2 hours at room temperature. Each slice was imaged under a confocal microscope (Olympus).

Behavioral tests

All behavioral tests were conducted in a sound attenuation booth during the dark cycle of the mice with dim ambient light. To test potential sex dimorphism, an equal number of animals of each sex were used. Because no difference in mPOA induced anxiety was observed between males and females, only male animals were used for later inactivation experiments and manipulations of downstream targets. 72 h gap was applied if the same animal was tested for multiple behavioral sessions.

Aversive stimulation application.—Animals were exposed to cold water (15°C), heat plate (50°C), or electrical foot shocks (0.3 mA, 0.5 Hz, 20-ms pulse duration) for 5min. Anxiety-related behavior test was performed 1h after the treatment.

Open field test.—A white behavior test box (60cm x 60cm x 30cm, length x width x height) was virtually divided into a center field (center, 30 x 30 cm) and a periphery field. For each test, the mouse was placed in the periphery and the locomotion of the animal was recorded by a video camera for 20 min to measure the time spent in the center or peripheral area.

Elevated plus maze test.—A crossed maze with two closed and two open arms was elevated 30cm above the ground. The mouse was placed in the center of the crossed maze and the locomotion of the animal was recorded by a video camera for 5 min.

Real-time place preference test.—A clear acrylic behavior box (40cm x 20cm x 20cm, divided into two chambers, put in a larger white foam box) with normal bedding materials was used. For each trial, the mouse was initially placed in the non-stimulation chamber, and LED (480 nm, 10 Hz, 5-ms pulse duration) stimulation was constantly delivered once the animal entered the stimulation chamber and was stopped when the animal exited. The total duration of each test session was 20 min. Animals were returned to their home cage after each test session. The stimulation chamber was randomly assigned to each animal and balanced for the whole group. We recorded the behavioral data via a web camera. The LED stimulation was automatically close-loop controlled by customized software (written by Guang-Wei Zhang, in Python 3.4) which detects the location of the animal in real-time. The online analysis is as described below.

Conditioned place preference test.—A clear acrylic behavior box (40cm x 20cm x 20cm, put in a larger foam box) was divided into three chambers. The middle chamber has a grey smooth metal plate floor, the left chamber has white walls and a grid-wire floor, and the right chamber has black walls and a parallel-wire floor. On day 1, each animal was placed in the middle chamber, and no preference towards either left or right chamber was observed. The black or white chamber was then assigned randomly as the stimulation chamber for that animal. On the 2nd and 3rd day, the animal was confined into the stimulation chamber for 20 min while LED stimulation was applied. And 4 hours later it was also placed in the other chamber with no treatment for 20 min. On day 4, the animal was placed in the middle chamber and could freely get access to all chambers.

Shelter time test.—A clear acrylic behavior box (20cm x 20 cm x 20cm) novel to the testing animal was used. A triangular shelter was placed at the corner. Animal was placed in the chamber and locomotion was recorded by a camera. The percentage of time spent in the shelter and outside the shelter was off-line analyzed using the object-detection software described below.

Dark-light box test.—An acrylic behavior box (40cm x 20cm x 20cm) was divided into a dark chamber (10cm x 20cm x 20cm) and a light chamber (30cm x 20cm x 20cm). The dark chamber was shielded with black aluminum foil. Animal was placed in the light side at the

beginning and the behavior were recorded by a camera. The time spent on the light side was analyzed using the object-detection software described below.

Pup-directed aggression test.—Virgin male mice were housed individually for 5 days before behavioral tests. The test was conducted in the home cage of the virgin male. After 30 min habituation, one C57/BL6 pup (< 4 days) was introduced to the far-side corner relative to the nest in the home cage. One trial would be defined as attack trial if the virgin male bit the pup within 15min. Grooming is defined as the sniffing and licking of the pup. LED stimulation was applied once the male started exploring the pup. Each trial would be terminated once the male bit the pup, and the pup would be immediately sacrificed. The LED ON and OFF trials are randomly assigned across different testing days, with 72h resting time in between. Each animal was tested for 1-3 trials and only 1 trial performed on a testing day.

Pup-induced anxiety test.—A foreign C57/BL6 pup (< 4 days) was introduced to the home cage of the virgin male. The pup was protected by using a transparent box with holes that would not block the pup odor or sound. The exposure lasted for 15 min and the virgin male was subjected to OFT and EPM tests right after the exposure.

Inter-male aggression test.—Virgin male mice were housed individually before the inter-male aggression test, which was conducted in the home cage of the virgin male (resident cage). The virgin male was briefly exposed to a female mouse for 1 h two days before the test. After 30 min habituation, a castrated younger male (4 weeks old) with wild-type male fresh urine odor was introduced to the resident cage. A trial would be defined as fighting trial if the resident virgin male bit the intruder mouse. LED ON and OFF trials were randomized across different testing days, with 72h resting time in between.

3D object dislocation test.—The testing animal was habituated to a clear acrylic behavior box (20cm x 20 cm x 20cm) for 15 min before test. A 3D novel object (2cm x 2cm x 2cm) was placed in the center of the chamber. After 3min LED OFF block, LED was applied for 3min (10Hz), followed by a 3min LED OFF block. The travelling distance of the 3D object was calculated offline using customized software (written by Guang-Wei Zhang, in Python 3.4).

Food intake test.—Mice were housed with food and water *ad libitum*. Just before the behavioral test, the animal was food deprived for 24h with water *ad libitum*. During a 2h test block, the animal gained access to food, and LED stimulation (10 Hz, 5-ms duration) was continuously applied. The weight of food consumed was measured after the test block. For chemogenetic manipulation, the test was started 20 min after the CNO injection (i.p.).

Thermoregulation test.—Core body temperature (anal temperature) was measured after 30-min optogenetic light stimulation (10Hz, 5 ms pulse duration).

Real-time animal detection and closed-loop optogenetic control

A customized mouse detection software was used for online real-time animal detection (written by Guang-Wei Zhang, in Python 3.4, www.python.org, with OpenCV library,

https://opencv.org)[27,52]. The behavior of the animal was monitored using an infrared camera at 24fps. Then each frame was gaussian blurred and then binarized. The gravity center for the detected contour was used to determine the location of each animal. In the two-chamber place preference test, the stimulation chamber was randomly assigned (balanced within the group) to each animal. Once the mouse entered the stimulation chamber, computer-controlled Arduino microcontroller (www.arduino.cc) would generate TTL signals to drive the LED light source (ThorLabs Inc.). The behavior test was run automatically without experimenter's interference and the result was calculated right after each experiment.

Pupil size measurement and off-line quantification

Animal was head-fixed. A CMOS camera (Point Grey, FL3-U3-13Y3M-C, equipped with Fujinon 1:1.4/9mm lens, HF9HA-1B) was used to capture images of the right eye. The ambient light was provided using a 13'' monitor (Dell, Inc.) at ~58lx illuminance. An infrared LED array was used to provide infrared illumination. The image acquisition (25 fps) was synchronized with the optogenetic LED stimulation via a computer with data acquisition card (National Instruments) using customized software (Written by Li Shen, in LabVIEW). The pupil size was offline analyzed (software written by Guang-Wei Zhang, in Python 3.4): each frame was Gaussian filtered and the black pupil was extracted using a threshold adjusted for each experiment. The nearest eclipse was fitted to estimate the diameter of the pupil. For each experiment, a few frames were dropped due to eye blink and the corresponding pupil size value was estimated using interpolation based on 5 frames before and after the eye blink.

Histology

Animals were sacrificed 3h after exposure to water (15°C), heat plate (50°C) or electrical foot shock (0.3 mA, 0.5 Hz, 20-ms pulse duration). For control experiments, animals were subjected to the same handling at room temperature, without shock or water (Fig. S1). The brain was fixed overnight and sectioned at 50 μm thickness. Immunohistochemistry was performed according to standard protocol with goat anti-c-fos (1:1000, Santa Cruz Biotechnology). For co-labelling of Vglut2 and c-fos expression, Vglut2-Cre::Ai14 transgenic animals were used.

Slice recording

To confirm the connectivity between mPOA glutamatergic axons and PAG neurons. Vglut2-*ires*-Cre mice injected with AAV2/1-pEF1α-DIO-hChR2-eYFP in mPOA were used for slice recording. Three weeks following the injections, animals were decapitated following urethane anesthesia and the brain was rapidly removed and immersed in an ice-cold dissection buffer (composition: 60 mM NaCl, 3 mM KCl, 1.25 mM NaH_2PO_4, 25 mM $NaHCO_3$, 115 mM sucrose, 10 mM glucose, 7 mM $MgCl_2$, 0.5 mM $CaCl_2$; saturated with 95% O_2 and 5% CO_2; pH = 7.4). Coronal slices at 350 μm thickness were sectioned by a vibrating microtome (Leica VT1000s), and recovered for 30 min in a submersion chamber filled with warmed (35°C) ACSF (composition:119 mM NaCl, 26.2 mM $NaHCO_3$, 11 mM glucose, 2.5 mM KCl, 2 mM $CaCl_2$, 2 mM $MgCl_2$, and 1.2 NaH_2PO_4, 2 mM Sodium Pyruvate, 0.5 mM VC). PAG neurons surrounded by $EYFP^+$ fibers were visualized under a fluorescence microscope (Olympus BX51 WI). Patch pipettes (~4–5 MΩ resistance) filled

with a cesium-based internal solution (composition: 125 mM cesium gluconate, 5 mM TEA-Cl, 2 mM NaCl, 2 mM CsCl, 10 mM HEPES, 10 mM EGTA, 4 mM ATP, 0.3 mM GTP, and 10 mM phosphocreatine; pH = 7.25; 290 mOsm) were used for whole-cell recordings. Signals were recorded with an Axopatch 700B amplifier (Molecular Devices) under voltage clamp mode at a holding voltage of −70 mV for excitatory currents, filtered at 2 kHz and sampled at 10 kHz. Tetrodotoxin (TTX, 1 μM) and 4-aminopyridine (4-AP, 1 mM) were added to the external solution for recording monosynaptic responses to blue light stimulation (5 ms pulse, 3 mW power, 10–30 trials). CNQX (20 μM, Sigma-Aldrich) was added to the external solution to block glutamatergic currents.

For testing the efficacies of ChR2, ArchT and hM4D(Gi), hM3D(Gq), brain slices were prepared similarly, and whole-cell current-clamp recordings were made from neurons expressing ChR2, ArchT, hM4D(Gi) or hM3D(Gq). A train of blue light pulses at different frequencies (1-20 Hz, 5-ms pulse duration) was applied to measure spike responses of ChR2-expressing neurons. Green light stimulation (10-s duration) was applied to measure hyperpolarization in ArchT-expressing neurons. For neurons expressing hM4D(Gi) or hM3D(Gq), spontaneous spikes were recorded before and after perfusion of CNO (10 μM) and after washing out CNO.

Cell-type specific monosynaptic retrograde tracing

To trace the monosynaptic input to Vglut2+ neurons in mPOA, AAV1-DIO-FLPo-WPRE-hGHpA, AAV8-CAG-fDIO-TVA-mCherry and AAV_{DJ}-CAG-fDIO-oG-WPRE were mixed (1:1:1, 80 nl) and stereotactically injected into mPOA of Vglut2-Cre mice. After two weeks, EnvA-G-deleted Rabies-GFP was injected in mPOA. The animal was sacrificed one week later. Brain tissue was fixed, sectioned and imaged using a confocal microscope.

Statistics

When it is possible, a prior power analysis was used to determine sample sizes. Otherwise, sample sizes were selected based on previous experience from related research or literature. Animals were randomly assigned to control and treatment groups. For the animals with multiple treatment, the sequence of treatment was randomized. Investigators were not blinded to group allocation or data collection, but the analyses of behavioral data were performed blind to the conditions of experiments as data obtained under different conditions were pooled together for an automatic batch analysis with computer softwares. Prism8 software (Graphpad) and R have been used for statistical analysis. Kolmogorov-Smirnov test were used to test normality. Mann-Whitney test was used for non-normality data. Kolmogorov-Smirnov test was used for comparing the response difference between shock exposed and control group. One-way ANOVA and Two-way ANOVA and post hoc Tukey's multiple comparisons were used to test significance between samples. For two-group comparison of normality data, significance was determined by using t-test. Paired t-test was used to compare data from the same animal. In this study, no data was excluded from analysis.

Extended Data

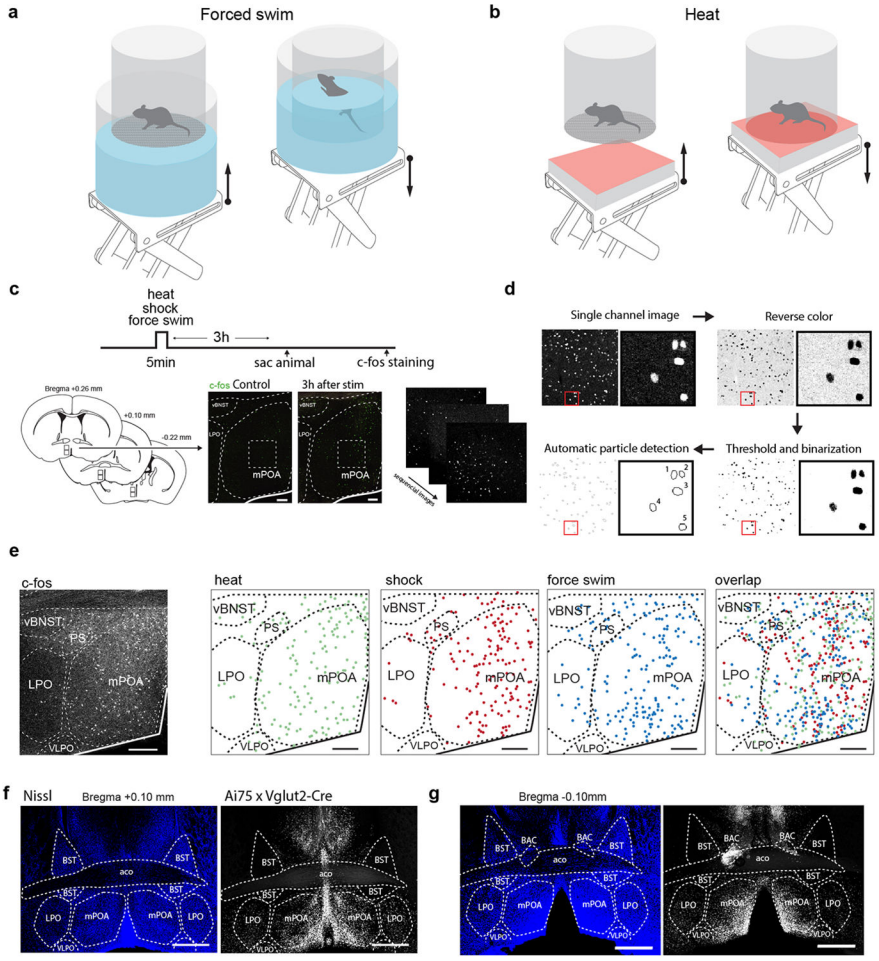

Extended Data Fig. 1. Quantification pipeline for c-fos staining and Vglut2 expression in mPOA. (Associated with Fig. 1)

a. Illustration of force swimming application. The bottom of the test chamber was a metal mesh. For the control experiment, the animal was placed in the same context without being submerged into water (condition on the left).

b. Illustration of heat plate application. For the control experiment, the animal was placed in the same context without being touched by the heat plate (condition on the left).

c. Protocol for c-fos staining and imaging. Animals were exposed to one of the stressors for 5 min and were sacrificed 3 hours after the treatment. Scale, 100 μm.

d. Pipeline for image processing and cell counting.

e. Spatial distribution of c-fos+ cells under treatments of three different stressors. LPO, lateral preoptic area; VLPO, ventral lateral preoptic area. Scale, 200 μm.

f. Left, Nissl staining; right, tdTomato expression in the same coronal brain section. Images were obtained from transgenic mice by crossing Ai75 (Cre-dependent nucleus-targeted tdTomato reporter) and Vglut2-Cre.

g. A more posterior section. BAC, bed nucleus of the anterior commissure; aco, anterior commissure. Scale, 500μm.

Images in **c,d** are representative of n = 9animals, Images in **e,f,g** are representative of n=3 animals.

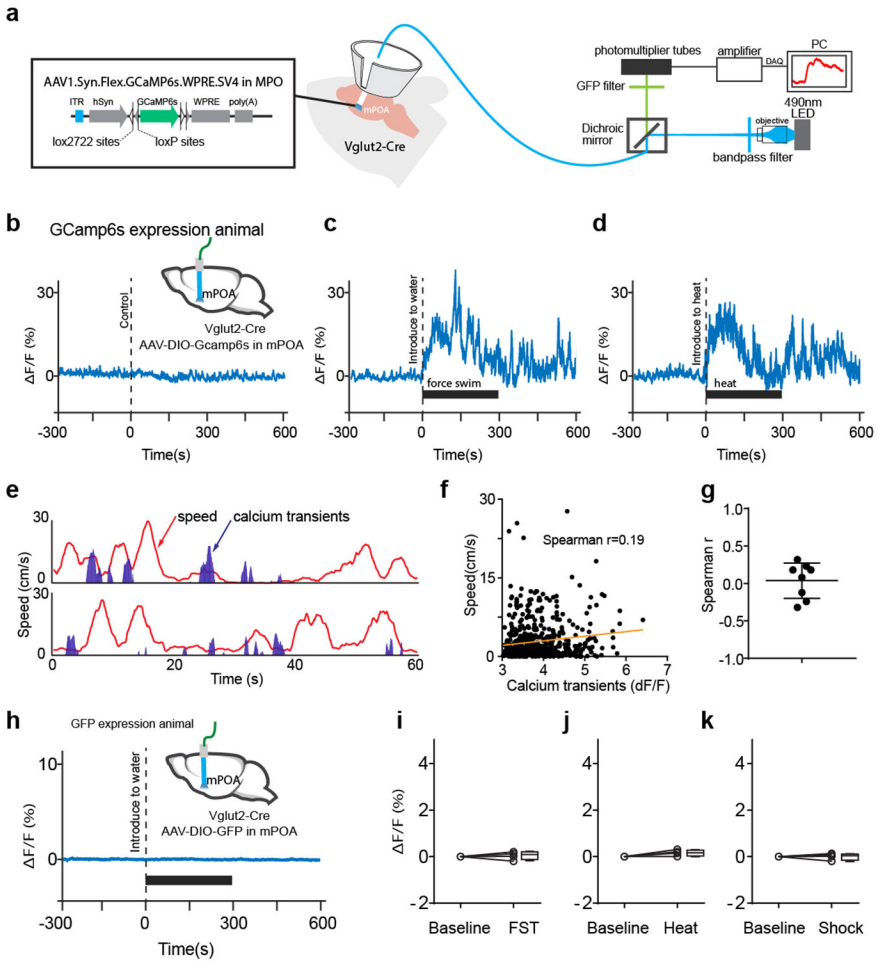

Extended Data Fig. 2. Quality control for fiber photometry. (Associated with Fig. 1)

a. Illustration of the fiber photometry setup. A protective cover helps to prevent the optic fiber from bumping against the wall of the test box/chamber. Neurons express Cre-dependent GCaMP6s.

b. Example full trace of calcium signals in the control condition for forced swimming. Dashed line indicates the presumptive operation time (no operation was actually applied).

c. Example full trace of calcium signals for forced swimming application. Bar represents the exposure duration.

d. Example full trace of calcium signals for heat plate application.

e. Plot of calcium transients (blue) and concurrent locomotion speed (red, freely moving) in an open field. Z-score = 3 was used as the detection threshold.

f. Plot of locomotion speed vs. amplitude of calcium transients.

g. Spearman *r* calculated for each mouse. N= 8 animals. Bars represent mean ± s.d.

h. Fluorescence signals in a control animal expressing GFP only. Black bar marks duration of forced swimming exposure.

i. Peak calcium transients during the baseline period and stressor application for GFP control animals (n = 4). Statistics can be found in Fig.1. FST, forced swimming test.
j. Heat plate exposure in GFP control animals (n = 4).
k. Electric shock exposure in GFP control animals (n = 4).
(see Supplementary Table 1 for detailed statistics).

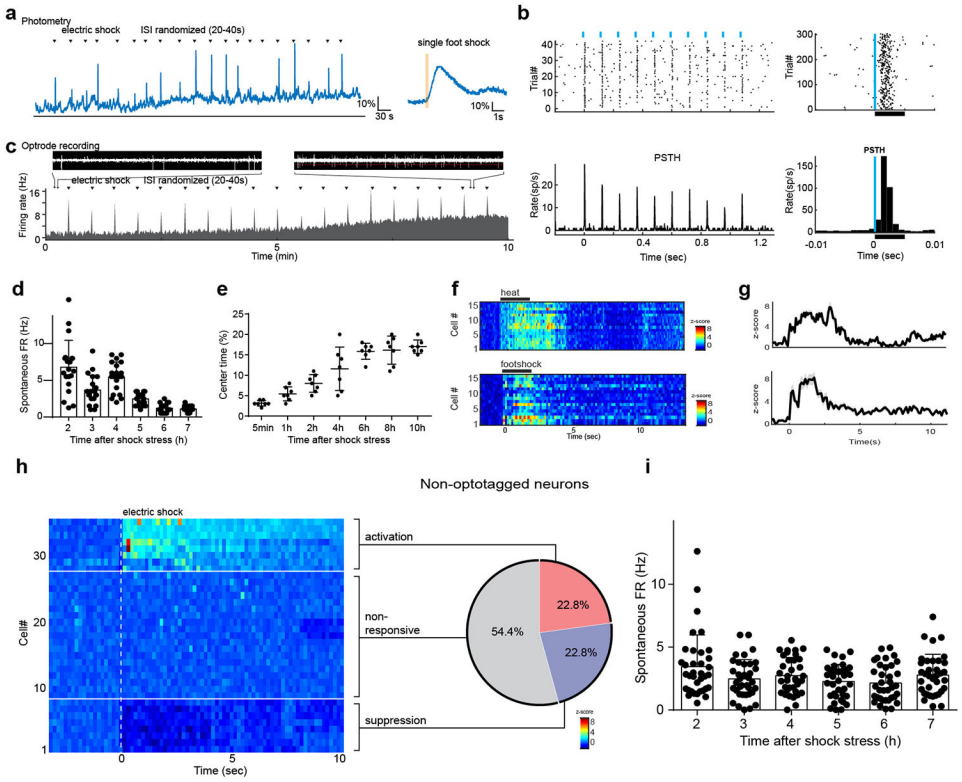

Extended Data Fig. 3. Optrode recording. (Associated with Fig. 1)
a. Top, example full trace of fiber photometry recording (left, each black dot represents one application of foot shocks) and average Ca^{2+} response (averaged over trials) to a foot shock application (right).
b. Top, raster plot of LED-induced spike responses for an example mPOA glutamatergic neuron. Blue dots indicate the duration of LED pulse (5ms). Bottom, corresponding peri-stimulus spike time histogram (PSTH). Raster plot and PSTH for spikes induced by a single LED pulse (blue line). Thick black line indicates the duration of LED stimulation. Only cells show 1st spike latency shorter than 4ms were considered as valid optogenetically-identified Vglut2+ neurons and included for analysis.
c. Example full trace of single-unit responses to repeated foot shock stimulation. Spontaneous spikes before the first and last electric shock application are shown on top for visualization.
d. Spontaneous firing rates of mPOA opto-IDed Vglut2+ neurons at different time points after exposure to foot shocks. N = 19 cells from 2 animals.
e. Center time in OFT performed at different time points after exposure to foot shocks. N = 7 animals.

f. Heatmaps of single-cell spike responses to heat (top) and electric shocks (bottom) of opto-IDed Vglut2+ neurons. The same cells are shown to demonstrate multimodal responses.
g. Population average of PSTHs from cells shown in (**f**).
h. Heatmap of single-cell spike responses to electric shocks for non-optotagged (presumably Vglut2−) neurons. Pie chart shows the percentage of presumably Vglut2− neurons that shows activated, no, or suppressive responses to electric shocks, respectively.
Spontaneous firing rates of non-optotagged neurons at different time points after exposure to foot shocks. N = 35 cells from 2 animals.

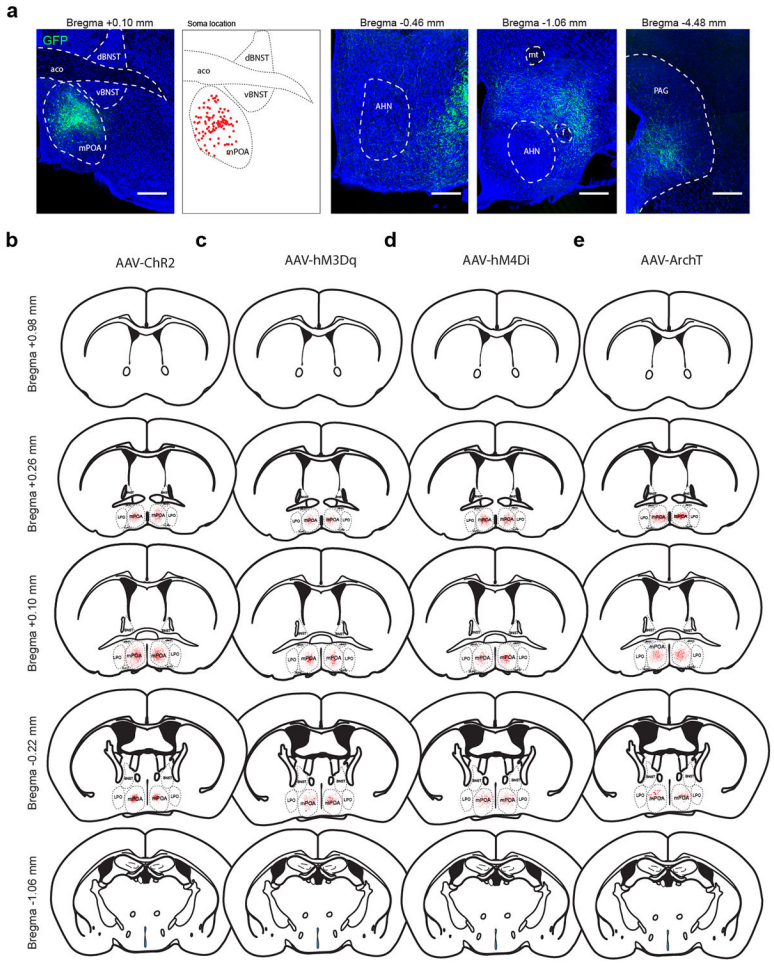

Extended Data Fig. 4. | Locations of somas with viral expression. (Associated with Fig. 2-4)
Schematic coronal sections ranging from 0.98 mm anterior to 1.06 mm posterior to Bregma.
a. Left two, Cre-dependent GFP expression at the injection site in a Vglut2-Cre mouse and spatial distribution of expressing cell bodies. Right three, axons in more posterior sections. Same image as in Fig. 5a. Blue, Nissl staining. Scale, 300μm.
b. . **a**, Representative images of GFP-labeled mPOA glutamatergic neurons (left) and their axons in PAG (right). Scale bar: 500 μm.
c. Superimposed ChR2-EYFP expressing cell locations for all mice from anterior to posterior sections. Each small red dot represents one cell.
d. Superimposed hM3Dq-mCherry expressing cell locations for all mice.

e. Superimposed hM4Di-mCherry expressing cell locations for all mice.
f. Superimposed ArchT-GFP expressing cell locations for all mice. Images in a are representative of n=6 animals.

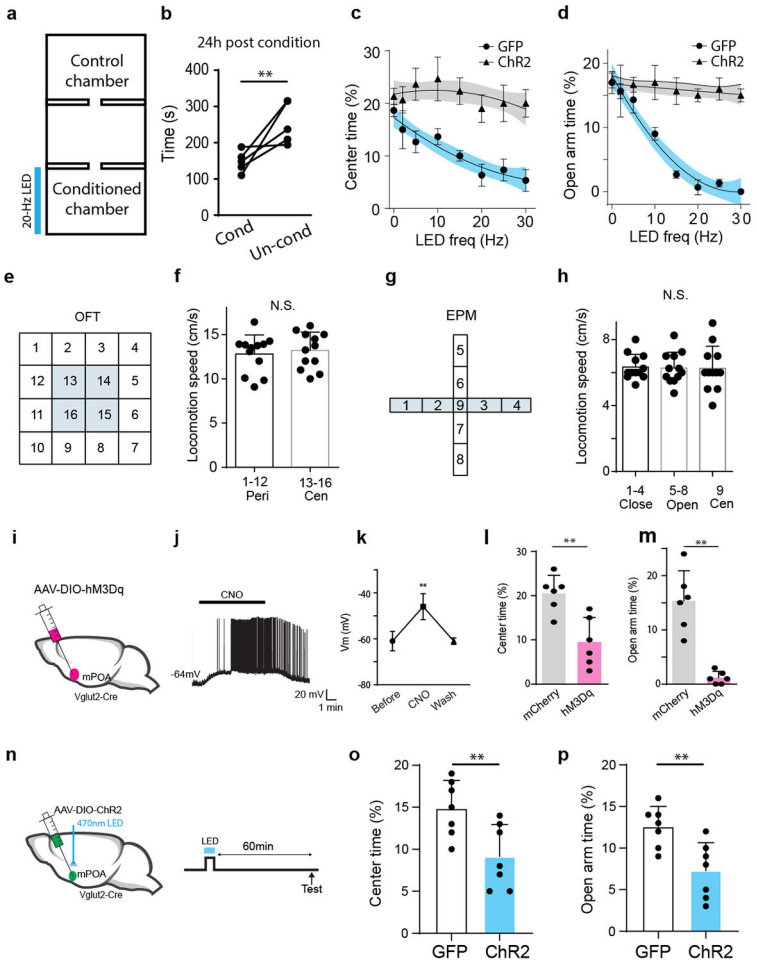

Extended Data Fig. 5. Activation of mPOA Vglut2 neurons. (Associated with Fig. 2)
a. Experimental setup for conditioned place preference test. During conditioning, the animal was subjected to LED stimulation whenever it was in the conditioned chamber.
b. Conditioned place aversion tested 24 hours after paring photo-stimulation with one chamber. Time spent in the conditioned chamber (Cond) or unconditioned chamber (Un-cond) was quantified. **P < 0.01, Mann–Whitney test, n = 5 animals.
c. Quantification of center time in OFT under different light stimulation frequencies (Kolmogorov–Smirnov test with Bonferroni correction, P < 0.001, n = 5 and 5 animals for GFP control and ChR2 groups respectively). Each animal was tested for one session per day with stimulation frequencies randomly selected.
d. Quantification of open-arm time in EPM (Kolmogorov–Smirnov test with Bonferroni correction, P < 0.001, n = 5 and 5 animals for GFP control and ChR2 groups respectively).
e. The OFT arena was divided into 16 subregions and locomotion speed were calculated for each specific subregion.

f. Locomotion speed in center vs peripheral subregions. Each dot is one animal. N.S., non-significant; paired t test. N=12.

g. The EPM arena was divided into 9 subregions.

h. Locomotion speed in closed-arm, open-arm and center subregions. N=12.

i. Expressing hM3Dq receptors in mPOA glutamatergic neurons.

j. Raw recorded trace of the membrane potential of a hM3Dq-expessing mPOA glutamatergic neuron in response to CNO application in slice recording.

k. Subthreshold membrane potential voltages before and after perfusion of CNO as well as after washing out CNO. **P < 0.01, one-way repeated-measures ANOVA, n = 5 cells from 2 animals.

l. Quantification of center time in OFT for mCherry control and hM3Dq expressing animals. **P < 0.01, Mann–Whitney test, n = 6 animals for each group.

m. Quantification of open-arm time in EPM for mCherry control and hM3Dq expressing animals. **P < 0.01, Mann–Whitney test, n = 6 animals for each group.

n. Experimental timeline: expressing ChR2 in mPOA glutamatergic neurons, optogenetic stimulation for 5-min (20Hz) and anxiety-related behavioral test one hour later.

o. Quantification of center time in OFT for GFP control and ChR2-expressing groups. **P < 0.01, Mann–Whitney test, n = 7 animals for each group.

Quantification of open arm time in EPM for GFP control and ChR2-expressing groups. **P < 0.01, Mann–Whitney test, n = 7 animals for each group. (see Supplementary Table 1 for detailed statistics).

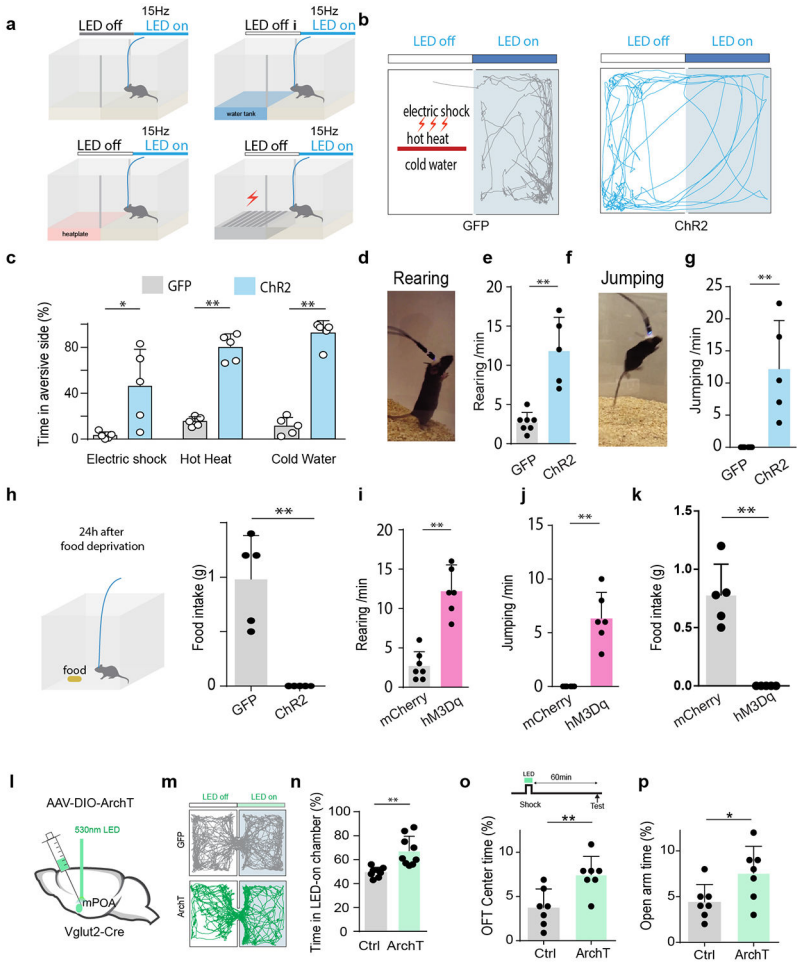

Extended Data Fig. 6. Strong activation of mPOA glutamatergic neurons. (Associated with Fig. 2)

a. Illustration of conflict tests.

b. Movement tracing of a GFP control animal (left) and a ChR2-expressing animal (right) in a conflict test. Photostimulation at 15 Hz was applied whenever the mouse was in the light gray marked zone.

c. Percentage time spent in the physically harmful side for control and ChR2 animals. *P < 0.05; **P < 0.01, Mann–Whitney test, n = 6 animals for each group.

d. Photo of mouse rearing during LED activation of mPOA glutamatergic neurons at 15Hz.

e. Frequency of rearing in GFP control (n = 7) and ChR2 expressing (n = 5) animals. **P < 0.01, Mann–Whitney test with Bonferroni correction.

f. Photo of mouse jumping during LED activation of nPOA glutamatergic neurons at 15Hz.

g. Frequency of jumping in GFP control (n = 7) and ChR2-expressing (n = 5) animals. **P < 0.01, Mann–Whitney test with Bonferroni correction.

h. Food intake within 2 hours after being food-deprived for 24 hours. During the 2h test, mPOA glutamatergic neurons were photo-stimulated continuously. **P < 0.01, Mann–Whitney test, n = 5 animals for each group.

i. Frequency of rearing in mCherry control (n = 7) and hM3Dq-expressing (n = 6) animals. **P < 0.01, Mann–Whitney test with Bonferroni correction.

j. Comparison of rearing frequency between mCherry control (n = 7) and hM3Dq-expressing (n = 6) animals. **P < 0.01, Mann–Whitney test with Bonferroni correction.
k. Food intake within 2 hours after being food-deprived for 24 hours. CNO injection (i.p.) was performed 20 min before the test. **P < 0.01, Mann–Whitney test with Bonferroni correction, n = 5 for each group.
l. Strategy of viral injection.
m. Movement tracing of a GFP control animal (upper) and an ArchT-expressing animal (lower) in a two-chamber place preference test. Continuous LED stimulation was applied whenever the animal stayed in the light gray marked chamber.
n. Percentage time spent in the LED-on chamber. **P<0.01, Mann-Whitney test, n = 9 (5 males) for each group.
o. Upper, experimental time line. LED light was applied only during the electric shocks. Center time in OFT for GFP control (n = 7) and ArchT-expressing (n = 7; 4 males) animals. **P < 0.01, Mann–Whitney test.
p. Open-arm time in EPM for GFP control (n = 7) and ArchT-expressing (n = 7; 4 males) animals. **P < 0.05, Mann–Whitney test, n = 7 animals for each group.
(see Supplementary Table 1 for detailed statistics).

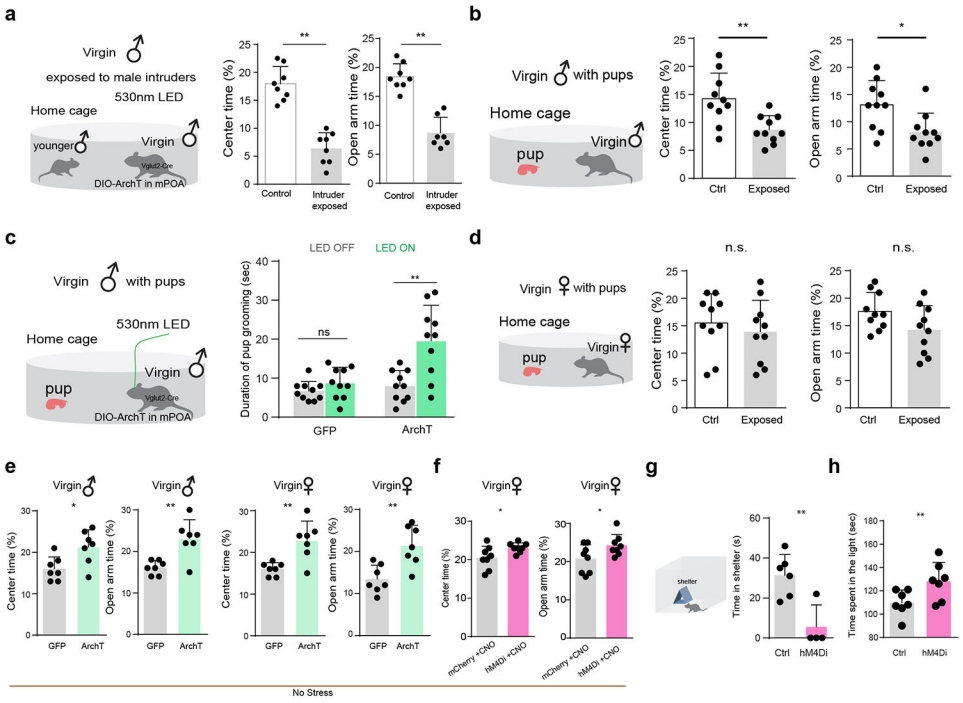

Extended Data Fig. 7. Anxiety tests after exposure to social stress. (Associated with Fig. 4)
a. Anxiety-like behaviors of virgin males with or without exposure to male intruders. **P < 0.01, Mann–Whitney test, n = 8 animals for each group.
b. Anxiety-like behaviors for virgin males with or without exposure to foreign pups. **P < 0.01, Mann–Whitney test, n = 10 animals for each group.
c. Duration of pup grooming for virgin males in LED-off and LED-on conditions. **P < 0.01, Mann–Whitney test with Bonferroni correction, n = 10 animals for each group.

d. Anxiety-like behaviors of virgin females with or without exposure to foreign pups. “n.s.”, not significant, Mann–Whitney test, n = 10 animals for each group.
e. Anxiety-related tests in virgin males/females not exposed to stress with (green) and without (grey) optogenetic silencing of mPOA Vglut2 neurons. *P < 0.05, **P < 0.01, Mann–Whitney test with Bonferroni correction, n = 7 animals for each group.
f. Anxiety-related tests in virgin females not exposed to stress with (green) and without (grey) chemogenetic silencing of mPOA Vglut2 neurons. **P < 0.01, Mann–Whitney test with Bonferroni correction, n =8 animals for each group.
g. Left, schematic open field test with a shelter. Right, total time spent in shelter within a 5-min test session. **P < 0.01, Mann–Whitney test, n = 6 (3 males) animals.
h. Total time spent in the light side of a light-dark box. **P < 0.01, Mann–Whitney test, n = 7 (4 males) animals for each group. (see Supplementary Table 1 for detailed statistics).

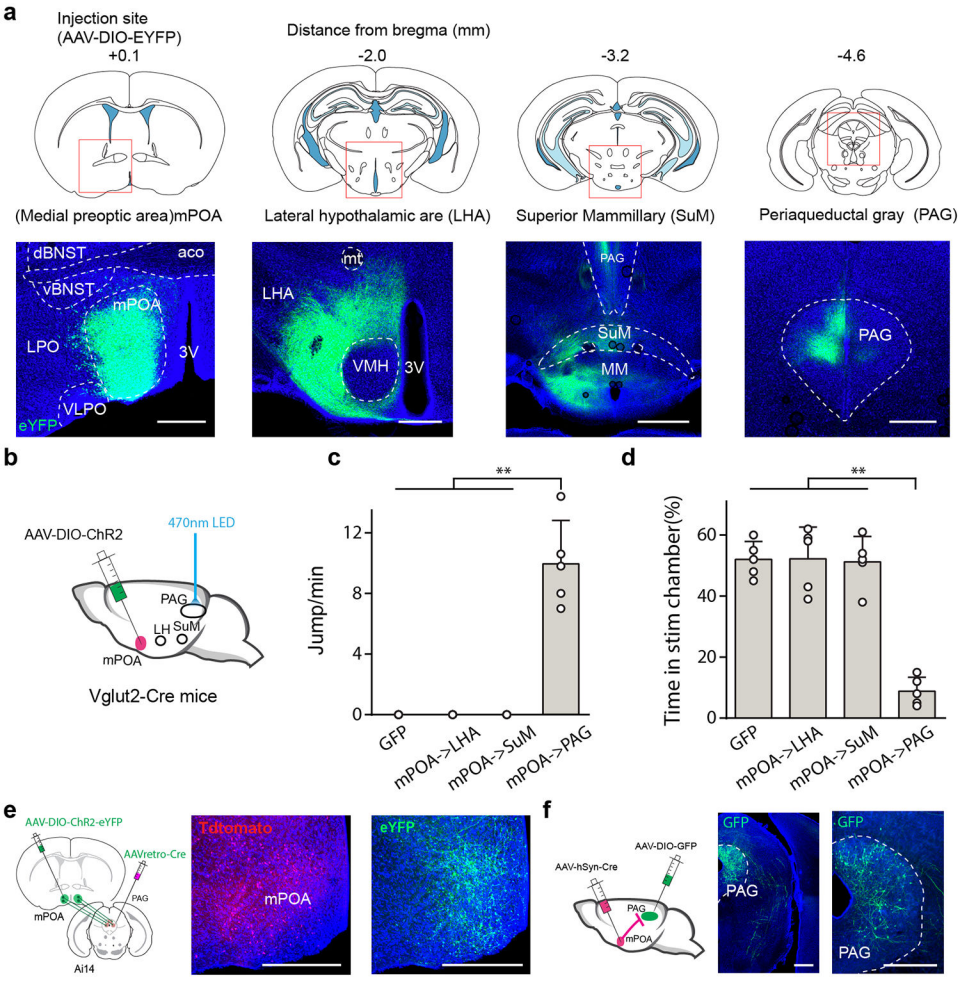

Extended Data Fig. 8. Potential targets of mPOA glutamatergic neurons. (Associated with Fig. 5)
a. Imaging area (top) and a confocal image (bottom) showing EYPF labeling in mPOA (left) and different downstream structures. Scale, 500μm. VMH, ventral medial hypothalamic nucleus; MM, medial mammillary nucleus.
b. Schematic terminal stimulation in a potential mPOA target.

c. Frequency of jumping induced by activating axonal terminals of mPOA glutamatergic neurons in different target areas. **P < 0.01, One-way ANOVA test, n = 5 animals for each group. GFP control group is for animals expressing GFP in mPOA with fiber implantation in mPOA.

d. Two-chamber place preference test when activating axonal terminals of MPO glutamatergic neurons in different target areas. **P < 0.01, One-way ANOVA test, n = 5 animals for each group.

e. Left, viral injection strategy to express ChR2 in PAG-projecting mPOA neurons in Ai14 mice. Right, images showing tdTomato- and ChR2-EYFP labeled neurons in mPOA. Scale bar, 500 μm.

f. Left, viral injection strategy to transsynaptically label mPOA-recipient PAG neurons. Right, image showing labeled neurons in PAG (with a blow-up image on the right). Scale bar, 500 μm.

Images in **a,e** are representative of n=5 animals. Images in **f** are representative of n =3 animals. (see Supplementary Table 1 for detailed statistics).

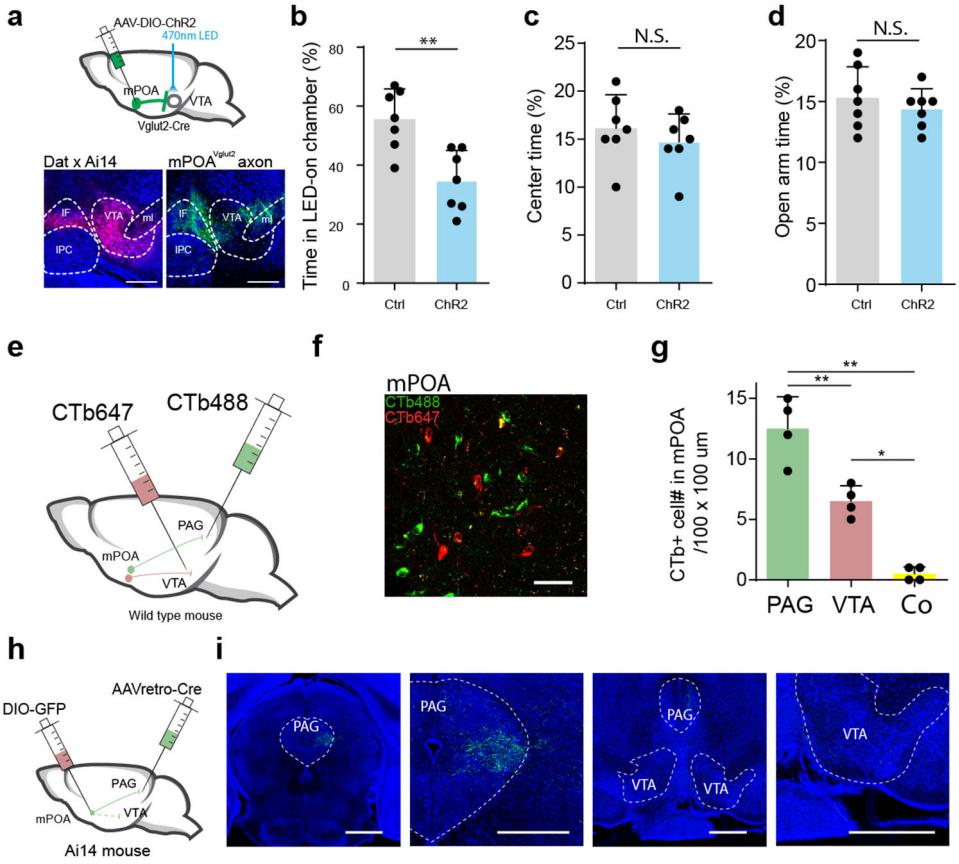

Extended Data Fig. 9. Manipulation of the mPOA to VTA pathway. (Associated with Fig. 5)

a. Top, viral injection strategy. Optic cannula was implanted above VTA. Bottom, labeling of dopamine neurons (red) by crossing DAT-Cre and Ai14 mice (left) and mPOA glutamatergic axons in VTA and surrounding regions (right). Scale, 400μm.

b. Percentage time spent in the LED-on chamber in PPT for GFP control and ChR2-expressing animals. **P<0.01, Mann-Whitney test, n = 7 (4 males) for each group.
c. Center time in OFT. N.S., no statistical difference, Mann–Whitney test, n = 7 animals for each group.
d. Open-arm time in EPM. Mann–Whitney test, n = 7 animals for each group.
e. Double retrograde dye injection in PAG (green) and VTA (red).
f. Representative image showing retrogradely labelled neurons in mPOA.
g. Quantification of singly and doubly labeled neurons in mPOA. N=4 animals.
h. Viral strategy to label axon collaterals of PAG-projecting mPOA neurons in VTA.
i. Images showing many labeled axons in PAG (left two), but extremely sparse axons in VTA (right two). Injection site is shown in Fig. 5b (shared blue channel as reference). Scale, 500μm.
Images in **a,i** are representative of n =3 animals, images in **f** are representative of n = 4 animals. (see Supplementary Table 1 for detailed statistics).

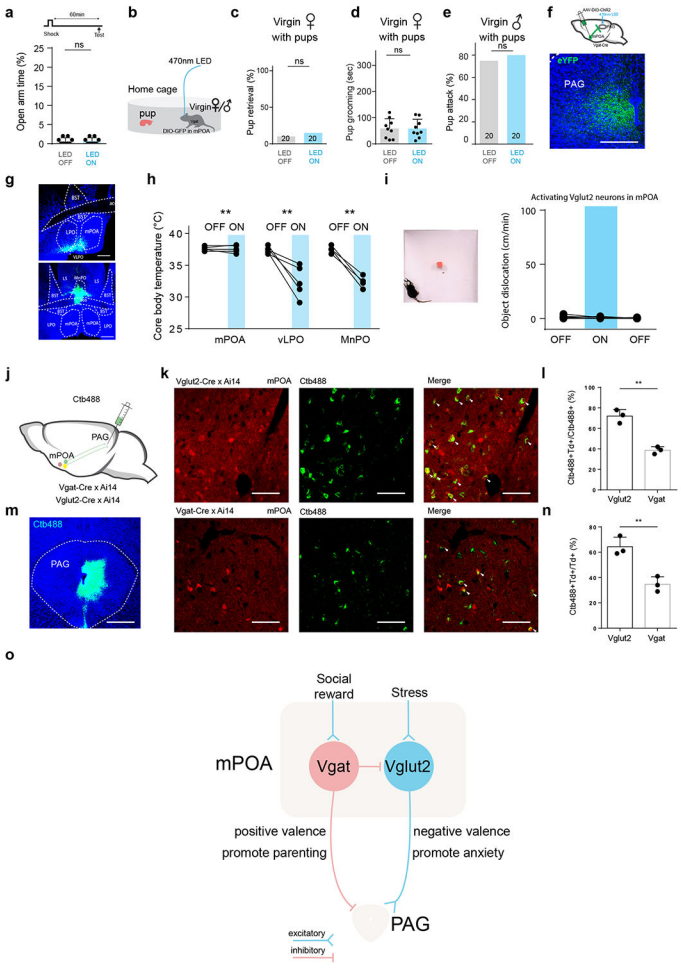

Extended Data Fig. 10. Control experiments for manipulating neurons in mPOA and proposed circuit model. (Associated with Fig. 6)

a. Open-arm time for GFP control animals in LED-off and LED-on conditions. “n.s.”, non-significant, Mann–Whitney test, n = 10 animals for each group.

b. Schematic pup exposure test for virgin males or females.
c. Percentage of trials with pup retrieval for GFP control virgin females in LED-on and LED-off conditions respectively. “n.s.”, non-significant, Fisher’s exact test, n = 7 animals for each group. Each animal was subjected to 2-4 trials and all trials were pooled together.
d. Duration of pup grooming for GFP control virgin females. “n.s.”, non-significant, Mann–Whitney test, n = 9 animals for each group.
e. Percentage of trials with pup attack for GFP control virgin males in LED-on and LED-off conditions respectively. “n.s.”, non-significant, Fisher’s exact test, n = 7 animals for each group. Each animal was subjected to 2-4 trials and all trials were pooled together.
f. Left, viral injection strategy and implantation of the optic fiber above PAG. Right, image showing axons of mPOA GABAergic neurons in PAG. Scale, 500 μm.
g. Representative images showing injection sites in VLPO (top) and MnPO (bottom). Scale, 500μm.
h. Core body temperature measured after 10-Hz LED stimulation for 30 min in animals expressing ChR2 in mPOA, ventral lateral preoptic area (vLPO) and median preoptic area (MnPO) respectively in Vglut2-Cre animals. **P < 0.01, two-tailed t-test, n = 5 animals for each group. bar, s.d.
i. Left, photo of a freely moving mouse in an open arena, with a 2x2x2cm 3D object placed in the center. The behavioral test consisted of 3 blocks: LED-off, LED-on, and then LED-off, with each lasting 3 min. 10-Hz LED stimulation was applied during the LED-on block. Right, dislocation of the 3D object by the mouse. No statistical significance was observed between blocks; two-way repeated-measures ANOVA, n = 5 animals.
j. CTb488 injection in PAG of either Vglut2-Cre::Ai14 or Vgat-Cre::Ai14 mice.
k. Images showing overlap between CTb-labeled and Vglut2+ (top) / Vgat+ (bottom) neurons in mPOA. Scale, 200 μm.
l. Quantification of the percentage of PAG-projecting mPOA neurons that are Vglut2+ or Vgat+. **P<0.01, Mann-Whitney test with Bonferroni correction, n = 3 animals for each group. Bar, s.d.
m. Representative image showing the CTb injection site in medial PAG.
n. Quantification of the percentage of Vglut2+ or Vgat+ mPOA neurons that were labeled by CTb injected in PAG. **P<0.01, Mann-Whitney test with Bonferroni correction, n = 3 animals for each group. Bar, s.d.
o. Illustration of the proposed circuit model. Note that due to potentially different inputs, glutamatergic neurons in mPOA respond to physical and social stressors but not to social rewards, while GABAergic neurons are activated by social rewards (e.g. during parenting) but not stressors.
Images in f are representative of n = 8 animals. Images in g are representative of n = 5 animals. Images in k, m are representative of n = 3 animals. (see Supplementary Table 1 for detailed statistics).

Supplementary Material

Refer to Web version on PubMed Central for supplementary material.

Acknowledgements

This work was supported by grants from the US National Institutes of Health to H.W.T. (EY019049; MH116990) and L.I.Z. (R01DC008983; RF1MH114112; MH116990). We would like to thank Y. Xiong and J. Wei in Southern Medical University for the generous help with behavioral experiments.

Data availability

All data that support the findings of this study are available from the corresponding authors upon request.

References

1. Calhoon GG & Tye KM Resolving the neural circuits of anxiety. Nat. Neurosci 18, 1394–1404 (2015). [PubMed: 26404714]
2. Craske MG & Stein MB Anxiety. Lancet 388, 3048–3059 (2016). [PubMed: 27349358]
3. Tovote P, Fadok JP & Lüthi A Neuronal circuits for fear and anxiety. Nat. Rev. Neurosci 16, 317–331 (2015). [PubMed: 25991441]
4. Fenster RJ, Lebois LAM, Ressler KJ & Suh J Brain circuit dysfunction in post-traumatic stress disorder: from mouse to man. Nat. Rev. Neurosci 19, 535–551 (2018). [PubMed: 30054570]
5. Merikangas KR et al. Longitudinal trajectories of depression and anxiety in a prospective community study: The Zurich cohort study. Arch. Gen. Psychiatry 60, 993 (2003). [PubMed: 14557144]
6. Adhikari A Distributed circuits underlying anxiety. Front. Behav. Neurosci 8, 112 (2014). [PubMed: 24744710]
7. Tye KM et al. Amygdala circuitry mediating reversible and bidirectional control of anxiety. Nature 471, 358–362 (2011). [PubMed: 21389985]
8. Jennings JH et al. Distinct extended amygdala circuits for divergent motivational states. Nature 496, 224–228 (2013). [PubMed: 23515155]
9. Kim SY et al. Diverging neural pathways assemble a behavioural state from separable features in anxiety. Nature 496, 219–223 (2013). [PubMed: 23515158]
10. Anthony TE et al. Control of stress-induced persistent anxiety by an extra-amygdala septohypothalamic circuit. Cell 156, 522–536 (2014). [PubMed: 24485458]
11. Padilla-Coreano N et al. Hippocampal-Prefrontal Theta Transmission Regulates Avoidance Behavior. Neuron 104, 601–610 (2019). [PubMed: 31521441]
12. Felix-Ortiz AC, Burgos-Robles A, Bhagat ND, Leppla CA & Tye KM Bidirectional modulation of anxiety-related and social behaviors by amygdala projections to the medial prefrontal cortex. Neuroscience 321, 197–209 (2016). [PubMed: 26204817]
13. Adhikari A, Topiwala MA & Gordon JA Synchronized Activity between the Ventral Hippocampus and the Medial Prefrontal Cortex during Anxiety. Neuron 65, 257–269 (2010). [PubMed: 20152131]
14. Wichmann R et al. Acute stress induces long-lasting alterations in the dopaminergic system of female mice. bioRxiv (2017). doi:10.1101/168492
15. Wei YC et al. Medial preoptic area in mice is capable of mediating sexually dimorphic behaviors regardless of gender. Nat. Commun 9, 279 (2018). [PubMed: 29348568]
16. Xu X et al. Modular genetic control of sexually dimorphic behaviors. Cell 148, 596–607 (2012). [PubMed: 22304924]
17. Dulac C, O'Connell LA & Wu Z Neural control of maternal and paternal behaviors. Science (80-.) 345, 765–770 (2014).
18. Fang YY, Yamaguchi T, Song SC, Tritsch NX & Lin D A Hypothalamic Midbrain Pathway Essential for Driving Maternal Behaviors. Neuron 98, 192–207 (2018). [PubMed: 29621487]
19. Wu Z, Autry AE, Bergan JF, Watabe-Uchida M & Dulac CG Galanin neurons in the medial preoptic area govern parental behaviour. Nature 509, 325–330 (2014). [PubMed: 24828191]

20. McHenry JA et al. Hormonal gain control of a medial preoptic area social reward circuit. Nat. Neurosci 20, 449–458 (2017). [PubMed: 28135243]
21. Carola V, D'Olimpio F, Brunamonti E, Mangia F & Renzi P Evaluation of the elevated plus-maze and open-field tests for the assessment of anxiety-related behaviour in inbred mice. Behav. Brain Res 134, 49–57 (2002). [PubMed: 12191791]
22. Ahrens S et al. A central extended amygdala circuit that modulates anxiety. J. Neurosci 38, 5567–5583 (2018). [PubMed: 29844022]
23. Xiu J et al. Visualizing an emotional valence map in the limbic forebrain by TAI-FISH. Nat. Neurosci 17, 1552–1559 (2014). [PubMed: 25242305]
24. Luo L, Callaway EM & Svoboda K Genetic Dissection of Neural Circuits: A Decade of Progress. Neuron 98, 256–281 (2018). [PubMed: 29673479]
25. Liu Z et al. Dorsal raphe neurons signal reward through 5-HT and glutamate. Neuron 81, 1360–1374 (2014). [PubMed: 24656254]
26. Hu H Reward and Aversion. Annu. Rev. Neurosci 39, 297–324 (2016). [PubMed: 27145915]
27. Zhang GW et al. Transforming Sensory Cues into Aversive Emotion via Septal-Habenular Pathway. Neuron 99, 1016–1028 (2018). [PubMed: 30122379]
28. Breton-Provencher V & Sur M Active control of arousal by a locus coeruleus GABAergic circuit. Nat. Neurosci 22, 218–228 (2019). [PubMed: 30643295]
29. Neumann ID, Veenema AH & Beiderbeck DI Aggression and anxiety: Social context and neurobiological links. Front. Behav. Neurosci 4, 12 (2010). [PubMed: 20407578]
30. Bluett RJ et al. Central anandamide deficiency predicts stress-induced anxiety: Behavioral reversal through endocannabinoid augmentation. Transl. Psychiatry 4, e408 (2014). [PubMed: 25004388]
31. Wang L et al. The coding of valence and identity in the mammalian taste system. Nature 558, 127–131 (2018). [PubMed: 29849148]
32. Zingg B et al. AAV-Mediated Anterograde Transsynaptic Tagging: Mapping Corticocollicular Input-Defined Neural Pathways for Defense Behaviors. Neuron 93, 33–47 (2017). [PubMed: 27989459]
33. Zhu Y, Wienecke CFR, Nachtrab G & Chen X A thalamic input to the nucleus accumbens mediates opiate dependence. Nature 530, 219–222 (2016). [PubMed: 26840481]
34. Moffitt JR et al. Molecular, spatial, and functional single-cell profiling of the hypothalamic preoptic region. Science (80-.) 362, eaau5324 (2018).
35. Callaway EM & Luo L Monosynaptic circuit tracing with glycoprotein-deleted rabies viruses. J. Neurosci 35, 8979–8985 (2015). [PubMed: 26085623]
36. Kim J et al. Rapid, biphasic CRF neuronal responses encode positive and negative valence. Nat. Neurosci 22, 576–585 (2019). [PubMed: 30833699]
37. Davis M, Walker DL, Miles L & Grillon C Phasic vs sustained fear in rats and humans: Role of the extended amygdala in fear vs anxiety. Neuropsychopharmacology 35, 105–135 (2010). [PubMed: 19693004]
38. Parfitt GM et al. Bidirectional Control of Anxiety-Related Behaviors in Mice: Role of Inputs Arising from the Ventral Hippocampus to the Lateral Septum and Medial Prefrontal Cortex. Neuropsychopharmacology 42, 1715–1728 (2017). [PubMed: 28294135]
39. McHenry JA, Rubinow DR & Stuber GD Maternally responsive neurons in the bed nucleus of the stria terminalis and medial preoptic area: Putative circuits for regulating anxiety and reward. Front. Neuroendocrinol 38, 65–72 (2015). [PubMed: 25910426]
40. Oh SW et al. A mesoscale connectome of the mouse brain. Nature 508, 207–214 (2014). [PubMed: 24695228]
41. Park SG et al. Medial preoptic circuit induces hunting-like actions to target objects and prey. Nat. Neurosci 21, 364–372 (2018). [PubMed: 29379117]
42. Chung S et al. Identification of preoptic sleep neurons using retrograde labelling and gene profiling. Nature 545, 477–481 (2017). [PubMed: 28514446]
43. Zhao ZD et al. A hypothalamic circuit that controls body temperature. Proc. Natl. Acad. Sci. U. S. A 114, 2042–2047 (2017). [PubMed: 28053227]

44. Papadimitriou GN & Linkowski P Sleep disturbance in anxiety disorders. Int. Rev. Psychiatry 17, 229–236 (2005). [PubMed: 16194794]
45. Tye KM Neural Circuit Motifs in Valence Processing. Neuron 100, 436–452 (2018). [PubMed: 30359607]
46. Glasheen C, Richardson GA & Fabio A A systematic review of the effects of postnatal maternal anxiety on children. Arch. Womens. Ment. Health 13, 61–74 (2010). [PubMed: 19789953]
47. Hård E & Hansen S Reduced fearfulness in the lactating rat. Physiol. Behav 35, 641–643 (1985). [PubMed: 4070441]
48. Lonstein JS Regulation of anxiety during the postpartum period. Front. Neuroendocrinol 28, 115–141 (2007). [PubMed: 17604088]
49. Kohl J et al. Functional circuit architecture underlying parental behaviour. Nature 556, 326–331 (2018). [PubMed: 29643503]
50. Dong HW, Petrovich GD & Swanson LW Topography of projections from amygdala to bed nuclei of the stria terminalis. Brain Res. Rev 38, 192–246 (2001). [PubMed: 11750933]

Methods References

51. Tervo DGR et al. A Designer AAV Variant Permits Efficient Retrograde Access to Projection Neurons. Neuron 92, 372–382 (2016). [PubMed: 27720486]
52. Zhang G, Shen L, Li Z, Tao HW & Zhang LI Track-Control, an automatic video-based real-time closed-loop behavioral control toolbox. bioRxiv (2019). doi:10.1101/2019.12.11.873372.

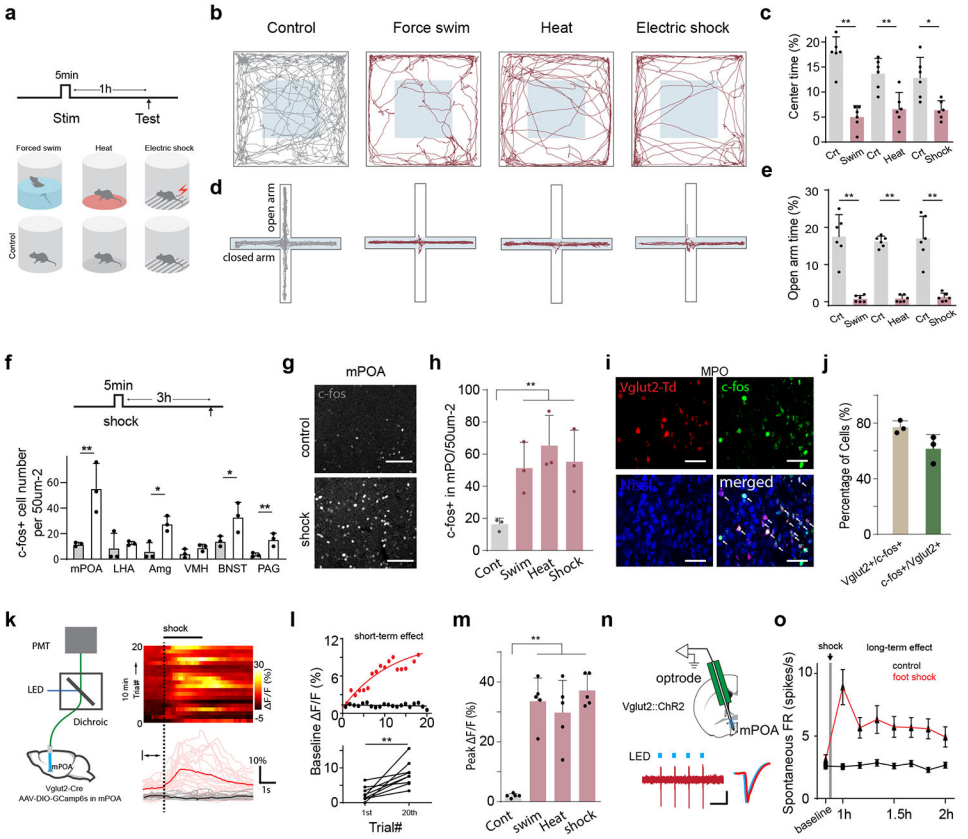

Fig. 1|. mPOA glutamatergic neurons are activated by physical stress.

a, Experimental timeline for measuring anxiety-like behaviors following 5-min treatment of either forced swimming, heat plate, or 0.5-Hz 0.3-mA electric shocks. **b**, Tracing of locomotion for representative control (gray) and experimental (dark red) animals exposed to different stressors. Light gray square marks the designated center zone. **c**, Quantification of percentage time spent in the center zone in OFT (n = 6 animals for each group, 3 males, 3 females; *P<0.05, **P < 0.01, two-way ANOVA and post hoc test). **d**, Locomotion traces for representative control and stressor-exposed animals. Light gray marks closed arms. **e**, Quantification of percentage time spent in the open arms of EPM (n = 6 animals for each group, 3 males, 3 females; ** P < 0.01, two-way ANOVA and post hoc test). **f**, Quantification of the number of c-fos+ cells per 50 μm^2 in different brain regions. mPOA, medial preoptic area; LHA, lateral hypothalamic area; Amg, amygdala; VMH, ventromedial hypothalamus; BNST, bed nucleus of the stria terminalis; PAG, periaqueductal gray. *P<0.05, **P < 0.01, two-way ANOVA and post hoc test, n = 3 animals. Top inset, experimental timeline for c-fos staining. **g**, Representative confocal images of c-fos staining in mPOA for a control and an experimental animal exposed to electric shocks. Scale bar: 50 μm. **h**, Quantification of number of c-fos+ neurons in mPOA for each treatment (n = 3 animals for each group; **P < 0.05, one-way ANOVA and post hoc test; control animals were combined). **i**, Representative images showing colocalization of Vglut2 (reflected by tdTomato expression in Vglut2-Cre::Ai14 mice) and c-fos (green) signals. Blue is Nissl staining. Scale bar: 25 μm. **j**, Quantification of percentage of Vglut2+ cells in the c-fos+ population (brown) and percentage of c-fos+ cells in the Vglut2+ population (green). **k**,

Left, experimental setup for photometry. Right, heatmap of Ca^{2+} signals to 20 trials of electric shocks (duration marked by a thick dark line) for an example animal. Bottom panel shows the averaged trace for the shock (solid red) and control (solid black, with no current output) condition, with pale colors indicating individual trials. Dashed line marks the onset of shocks. **l**, Top, baseline fluorescence signals within 1-s window just before the shock onset over 20 trials (red) for the same animal shown in **k**. Black is for a control animal. $P < 0.001$, Kolmogorov–Smirnov test with Bonferroni correction. Bottom, baseline fluorescence signal at the 1^{st} and 20^{th} trials for 9 animals. $^{**}P < 0.01$, two-sided paired t test. **m**, Quantification of stressor-induced peak $\Delta F/F$ (%) for control and exposed animals (n = 5 for each group, 3 males, 2 females; $^{**}P < 0.01$, one-way ANOVA and post hoc test; control animals were combined). **n**, Top, diagram for optrode recording from mPOA in head-fixed Vglut2-Cre::ChR2 mice. Bottom, sample recorded traces of spiking of a ChR2-expressing mPOA glutamatergic neuron to pulses of LED stimulation (blue dots). Right inset, comparison of spike waveforms (slightly offset) spontaneous generated (red) and evoked by LED stimulation (blue) of the same unit. **o**, Spontaneous firing rates across time (bin size: 10 min) before and after exposure to electric shocks (marked by vertical gray bar). $P < 0.001$, two-sided Kolmogorov–Smirnov test with Bonferroni correction; n = 35 and 29 neurons for control and experimental groups respectively. Bars represent s.e.m. Images in **g** are representative of n=3 animals. Data in **l** is representative of n = 5 animals. (Extended Data Fig. 1; see Supplementary Table 1 for detailed statistics).

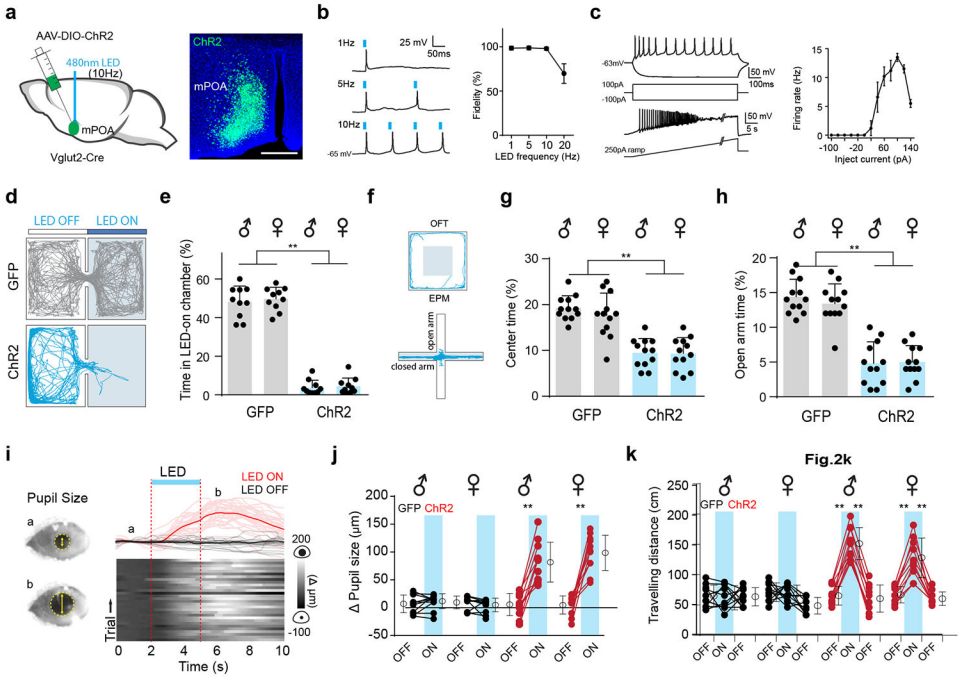

Fig. 2l. Activating mPOA glutamatergic neurons enhances anxiety-like behaviors.

a, Left, injection and stimulation configuration. Right, representative image showing expression of ChR2-EYFP in mPOA. Scale bar: 500 μm. **b**, Left, example traces of spiking of a recorded mPOA glutamatergic neuron to pulses of blue light at 1, 5 and 10 Hz. Right, fidelity of spiking at different stimulation frequencies (n = 10 cells). Bar = s.e.m. **c**, Left, example membrane potential responses to injections of square (upper) or ramp (lower) currents. Resting membrane potential was −63 mV. Right, average firing rates to injected currents at different amplitudes (n = 10 cells). Bar = s.e.m. **d**, Representative locomotion tracing for a GFP control and a ChR2-expressing animal in the two-chamber place preference test. **e**, Quantification of percentage time in the LED-on chamber. **P < 0.01, two-sided Mann–Whitney test with Bonferroni correction, n = 10 animals for each group. Males and females are separately displayed. Error bars, s.d. **f**, Locomotion tracing for an example ChR2-expressing animal with continuous photostimulation in OFT (upper) or EPM (lower). **g**, Quantification of center time in OFT. **P < 0.01, two-sided Mann–Whitney test with Bonferroni correction, n = 12 animals for each group. Error bars, s.d. **h**, Quantification of open-arm time in EPM. **P < 0.01, two-sided Mann–Whitney test with Bonferroni correction, n = 12 for each group. Error bars, s.d. **i**, Changes in pupil size in 60 trials of photostimulation (LED-on and LED-off trials were randomly assigned). Top, average change of pupil size in the LED-on (solid red) and LED-off (solid black) condition. Pale colors represent individual trials. Bottom, heatmap for change in pupil size in different trials aligned by the onset of LED stimulation (blue bar). Left inset, sample images of the eye at time points *a* and *b*. **j**, Average change in pupil size in LED-off and LED-on conditions. **P < 0.01, two-sided paired t-test, n = 11 animals for each group. Data points for the same animal are connected with a line. **k**, Traveling distance in an open arena in LED-off (3 min per block) and LED-on (3 min) conditions. **P < 0.01, two-way repeated-measures

ANOVA, n = 10 animals for each group. Images in **a** are representative of n=3 animals. (see Supplementary Table 1 for detailed statistics).

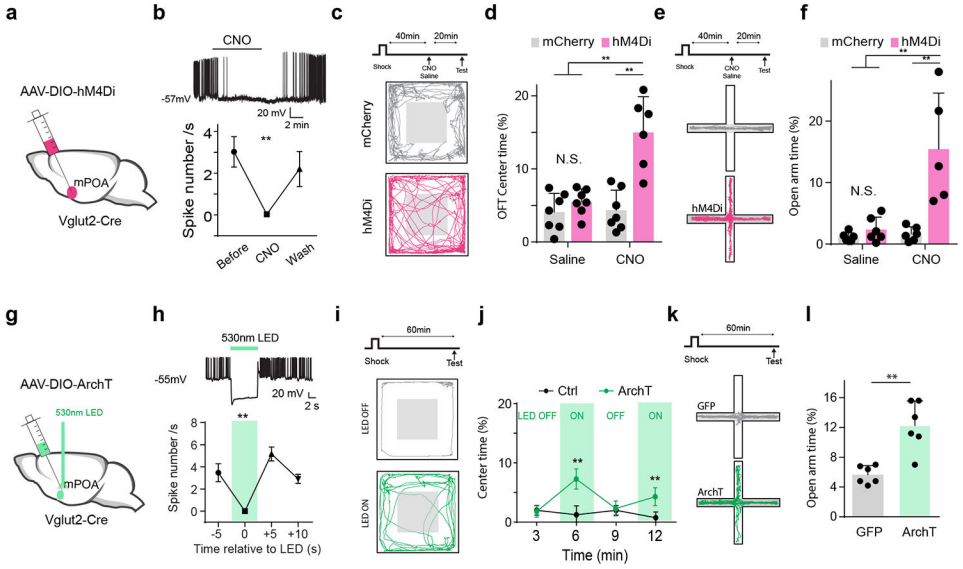

Fig. 3l. Silencing mPOA glutamatergic neurons reduces stress-induced anxiety-like behaviors.

a, Viral injection for chemogenetic silencing. **b**, Top, raw trace of current-clamp recording from a hM4Di-expressing mPOA glutamatergic neuron in the slice preparation. Bottom, average spontaneous spike frequencies before and after perfusion in of CNO as well as after washing out CNO. **P < 0.01, one-way repeated-measures ANOVA, n = 5 cells from 2 mice. Error bars, s.d. **c**, Movement tracing for an example mCherry control (gray) and a hM4Di-expressing (red) animal in OFT 1 hr after exposure to electric shocks, with CNO injected at 40 min. Top inset, experimental timeline. **d**, Percentage center time in OFT in mCherry control and hM4Di animals after shock exposure. **P < 0.01, two-sided Mann–Whitney test, n = 7 and 6 mice respectively, 3 males. Saline control experiments were performed on a different day for the same animal. Error bars, s.d. **e**, Movement tracing for a mCherry control (gray) and a hM4Di-expressing (red) animal in EPM test after exposure to electric shocks. **f**, Percentage open-arm time in EPM in mCherry control and hM4Di animals after shock exposure. **P < 0.01, two-sided Mann–Whitney test, n = 6 and 5 mice respectively, 3 males. Error bars, s.d. **g**, Viral injection and stimulation for optogenetic silencing. **h**, Top, membrane potential response to green LED stimulation in an ArchT-expressing mPOA glutamatergic neuron in the slice preparation. Bottom, average spontaneous spike rates before, during and after LED stimulation (marked by the green rectangle). **P < 0.01, one-way repeated-measures ANOVA, n = 5 cells from 2 mice. **i**, Movement tracing for an ArchT-expressing animal in OFT within a LED-off (gray) and a LED-on (green) block. **j**, Percentage center time for GFP control (black) and ArchT (green) animals in LED-off and LED-on blocks of OPT. **P < 0.01, two-way repeated-measures ANOVA, n = 8 and 9 animals (4 males) for control and ArchT groups respectively. Error bars, s.e.m. **k**, Movement tracing for a GFP control (gray) and an ArchT-expressing animal (green) in the EPM test. **l**, Percentage open-arm time for GFP control and ArchT animals. **P < 0.01, two-sided Mann–Whitney test, n = 6 animals (3 males) for each group. Error bars, s.d. (see Supplementary Table 1 for detailed statistics).

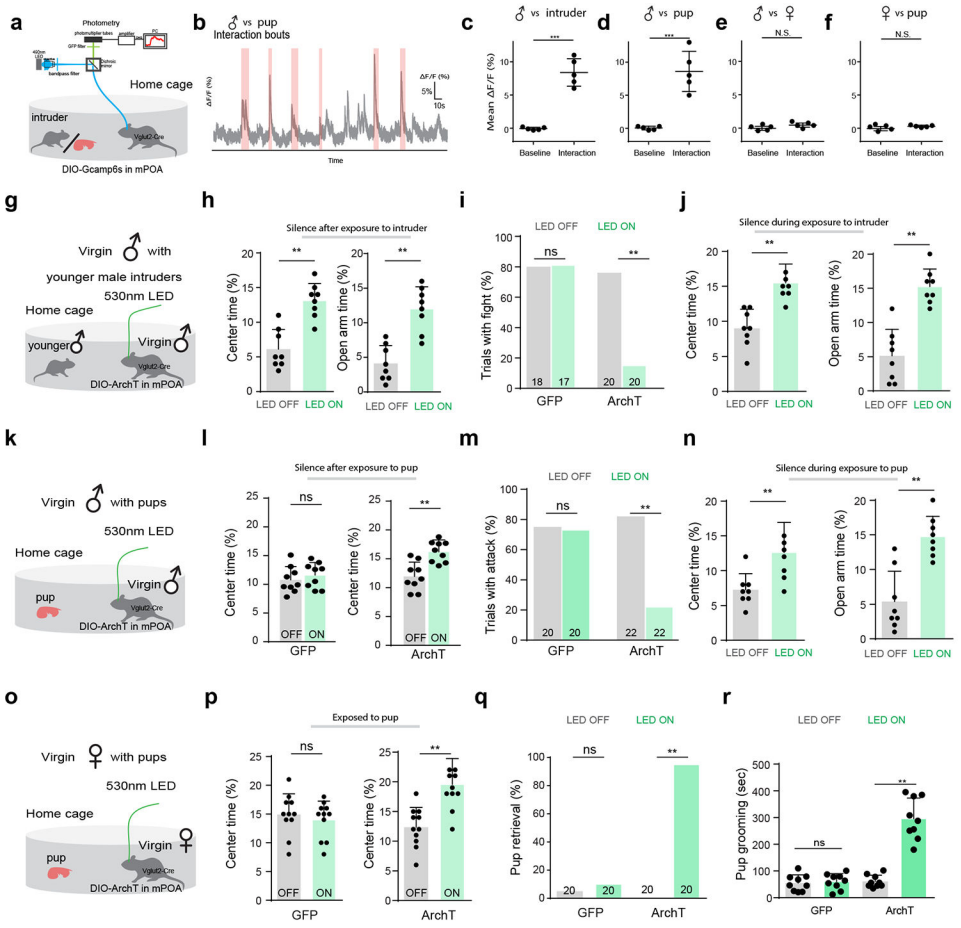

Fig. 4|. The mPOA glutamatergic neurons antagonistically regulate social stress-induced anxiety and parental behavior.

a, Exposing a resident mouse to a pup or a younger intruder while imaging ensemble Ca^{2+} activity of mPOA glutamatergic neurons using photometry. **b**, A representative trace for GCaMP6s fluorescence change in a virgin male when exposed to a pup. Colored bars indicate bouts of interaction with the pup. **c-e**, Percentage changes in fluorescence in virgin males before (pre-) and after (post-) putting in the home cage a male intruder (c), a pup (d) or a female (e). ***P < 0.01, two-sided Mann–Whitney test, n = 5 animals. Error bars, s.d. **f**, Percentage changes in fluorescence in virgin females (n = 5) before and after putting in a pup. Error bars, s.d. **g**, Experimental condition: a virgin male exposed to a younger male intruder. **h**, Percentage center time in OFT (left) and open-arm time in EPM (right) for intruder exposed resident males in LED-off (gray) and LED-on (green) conditions. **P < 0.01, two-sided Mann–Whitney test, n = 8 ArchT animals. Error bars, s.d. **i**, Percentage of trials with the resident fighting against intruder in LED-off (gray) and LED-on (green) conditions for GFP control and ArchT animals. **P < 0.01, two-sided Fisher's exact test with Bonferroni correction, n = 8 animals in each group; "ns", non-significant. Total number of trials is marked. **j**, Percentage center times in OFT (left) and open-arm times in EPM (right) without (gray) and with (green) optogenetic silencing of mPOA glutamatergic neurons during exposure to intruder. **P < 0.01, two-sided Mann–Whitney test, n = 8 ArchT animals. Error bars, s.d. **k**, Experimental condition: a virgin male exposed to a pup. **l**,

Percentage center times in OFT for GFP control (left, n = 9) and ArchT (right, n = 9) animals in LED-off (gray) and LED-on (green) conditions. **P < 0.01, Mann–Whitney test; “ns”, non-significant. Error bars, s.d. **m**, Percentage of trials with the virgin male showing pup attacks in LED-off and LED-on conditions for GFP (n = 9) and ArchT (n = 9) animals. **P < 0.01, Fisher’s exact test with Bonferroni correction. Total number of trials is marked. **n**, Percentage center times in OFT (left) and open-arm times in EPM (right) for pup-exposed males without (gray) and with (green) optogenetic silencing of mPOA glutamatergic neurons during pup exposure. **P < 0.01, Mann–Whitney test, n = 8 ArchT animals. Error bars, s.d. **o**, Experimental condition: a resident virgin female exposed to a pup. **p**, Percentage center times in OFT for GFP control (left, n = 11) and ArchT (right, n = 11) animals in LED-off (gray) and LED-on (green) conditions. **P < 0.01, Mann–Whitney test with Bonferroni correction. Error bars, s.d. **q**, Percentage of trials with pup retrieval for GFP (n = 11) and ArchT (n = 11) female mice in LED-off and LED-on conditions. **P < 0.01, Fisher’s exact test with Bonferroni correction. **r**, Total duration of pup grooming by the virgin female in LED-off and LED-on conditions. **P < 0.01, Mann–Whitney test with Bonferroni correction, n = 11 animals for both GFP and ArchT groups. Error bars, s.d. (see Supplementary Table 1 for detailed statistics).

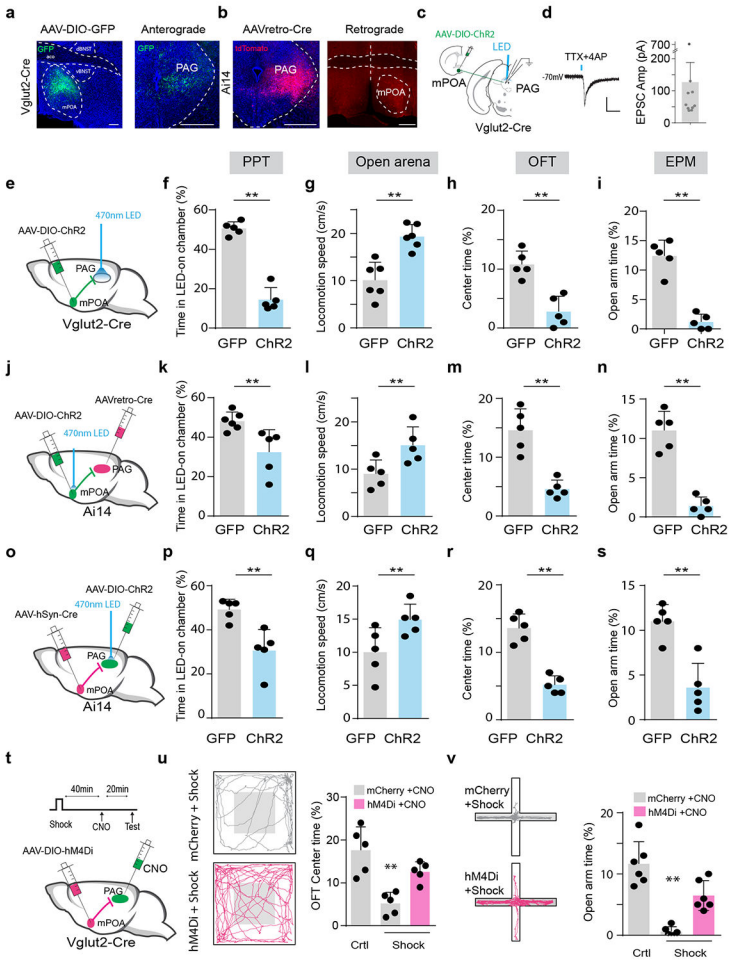

Fig. 5l. The mPOA to PAG pathway primarily accounts for the mPOA's role in regulating anxiety-like behaviors.

a, Representative images of GFP-labeled mPOA glutamatergic neurons (left) and their axons in PAG (right). Scale bar: 500 μm. **b**, Retrograde labeling of neurons in mPOA (right) by injection of AAVretro-Cre in PAG (left). Scale bar: 500 μm. **c**, Photoactivation of mPOA glutamatergic axons and recording from PAG neurons in the slice preparation. **d**, Left, voltage-clamp recording from a PAG neuron showing a light-evoked EPSC. Right, average amplitudes of light-evoked EPSCs in recorded PAG neurons (n = 10). Bar represents s.d. **e**, Photoactivation of mPOA glutamatergic axon terminals in PAG. **f**, Percentage time in the LED-on chamber in PPT. **P < 0.01, two-sided Mann–Whitney test, n = 5 animals for both GFP and ChR2 groups. Error bars, s.d. **g**, Average locomotion speed in an open arena. **P < 0.01, Mann–Whitney test, n = 6 animals for each group. Error bars, s.d. **h**, Percentage center time in OFT. **P < 0.01, Mann–Whitney test, n = 5 animals for each group. Error bars, s.d. **i**, Percentage open-arm time in EPM. **P < 0.01, two-sided Mann–Whitney test, n = 5 animals for each group. Error bars, s.d. **j**, Strategy to label PAG-projecting mPOA neurons with ChR2. Error bars, s.d. **k-n**, Similar to **f-i**, for photoactivation of PAG-projecting mPOA neurons. **P < 0.01, two-sided Mann–Whitney test, n = 5 or 6 animals for each group. Error bars, s.d. **o**, Strategy for photoactivation of mPOA-recipient PAG neurons. **p-s**, Similar to **f-i**, for photoactivation of mPOA-recipient PAG neurons. **P < 0.01, two-sided Mann–Whitney

test, n = 5 or 6 animals for each group. Error bars, s.d. **t**, Chemogenetic silencing of mPOA→PAG glutamatergic axon terminals and experimental timeline. **u**, Left, movement tracing for an example mCherry control (gray) and a hM4Di-expressing (red) animal in OFT after exposure to electric shocks. Right, percentage center times in OFT for mCherry control animals in the control condition (n = 5), control animals after shocks (n = 5) and hM4Di animals after shocks (n = 5). P = 0.0007, two-sided one-way ANOVA; **P < 0.01, post hoc test. Error bars, s.d. **v**, Left, movement tracing for a mCherry control (gray) and a hM4Di-expressing animal (red) in the EPM test after exposure to shocks. Right, percentage open-arm times in EPM for mCherry control animals in the control condition (n = 6), control animals after shocks (n = 6) and hM4Di animals after shocks (n = 6). P < 0.0001, two-sided one-way ANOVA; **P < 0.01, post hoc test. Error bars, s.d. Images in **a,b** are representative of n=6,3 animals. (see Supplementary Table 1 for detailed statistics).

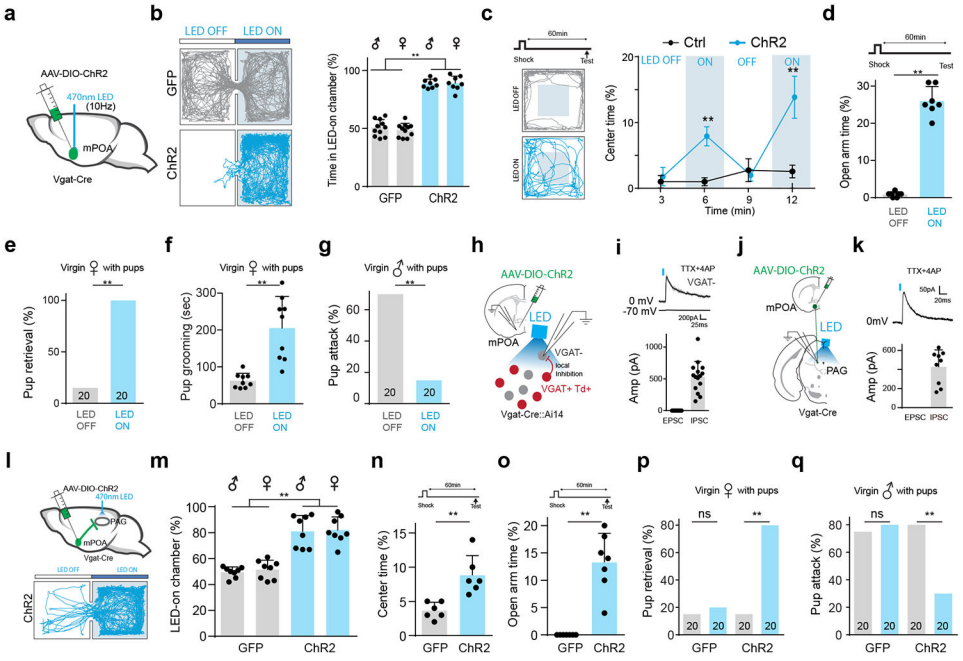

Fig. 6l. The GABAergic neurons play an opposite role in regulating anxiety state and parental behavior.

a, Expressing ChR2 in mPOA GABAergic neurons. **b**, Left, representative movement tracing of a GFP control (gray) and a ChR2 (blue) animal in PPT. Right, percentage times in the LED-on chamber for GFP (n = 11 males and 11 females) and ChR2 (n = 8 males and 8 females) mice. **P < 0.01, one-way repeated-measures ANOVA. Error bars, s.d. **c**, Left, movement tracing for a ChR2 animal in OFT within a LED-off (gray) and a LED-on (blue) block. Right, percentage center times for GFP control (black) and ChR2-expressing (blue) animals in LED-off and LED-on blocks. **P < 0.01, two-way repeated-measures ANOVA test, n = 7 animals (4 males) for each group. Error bars, s.d. **d**, Percentage open-arm times for ChR2 animals (n = 7; 4 males) in LED-off and LED-on conditions. **P < 0.01, two-sided Mann–Whitney test. Error bars, s.d. **e**, Percentage of trials with the virgin female exhibiting pup retrieval in LED-on and LED-off conditions. **P < 0.01, two-sided Fisher's exact test with Bonferroni correction, n = 7 ChR2 animals. **f**, Duration of pup grooming by the virgin female in LED-off and LED-on conditions. **P < 0.01, two-sided Mann–Whitney test with Bonferroni correction, n = 9 ChR2 animals. Error bars, s.d. **g**, Percentage of trials with the virgin males exhibiting pup attacks in in LED-off and LED-on conditions. **P < 0.01, two-sided Fisher's exact test with Bonferroni correction, n = 7 ChR2 animals. **h**, Recording from mPOA Vgat− neurons while stimulating Vgat+ neurons in the slice preparation. **i**, Top, traces of voltage-clamp recording from a mPOA glutamatergic neuron under two holding potentials. Blue vertical line indicates the onset of light stimulation. Bottom, average amplitudes of EPSCs and IPSCs in 15 mPOA glutamatergic neurons. Error bars, s.d. **j**, Recording from PAG neurons and photostimulation of ChR2-expressing GABAergic mPOA axons. **k**, Top, a light-evoked IPSC recorded in a PAG neuron. Bottom, average amplitudes of EPSCs and IPSCs from 9 PAG neurons. Error bars, s.d. **l**, Top, stimulation of GABAergic mPOA axons in PAG. Bottom, movement tracing of an example animal in PPT. **m**, Right, percentage times in the LED-on chamber for GFP and ChR2

animals. **P < 0.01, two-sided two-way repeated-measures ANOVA test, n = 8 animals for each group. Error bars, s.d. **n**, Percentage center times in OFT for GFP and ChR2 animals. **P < 0.01, two-sided Mann–Whitney test, n = 6 animals (3 males) for each group. Error bars, s.d. **o**, Percentage open-arm times in EPM for GFP and ChR2 animals. **P < 0.01, two-sided Mann–Whitney test, n = 7 animals (4 males) for each group. Error bars, s.d. **p**, Percentage of trials with the virgin female exhibiting pup retrieval in LED-off (gray) and LED-on (blue) conditions. **P < 0.01, two-sided Fisher's exact test with Bonferroni correction, n = 8 animals for both GFP and ChR2 groups. **q**, Percentage of trials with the virgin male exhibiting pup attacks in LED-off and LED-on conditions. **P < 0.01, two-sided Fisher's exact test with Bonferroni correction, n = 8 animals for both GFP and ChR2 groups. (see Supplementary Table 1 for detailed statistics).

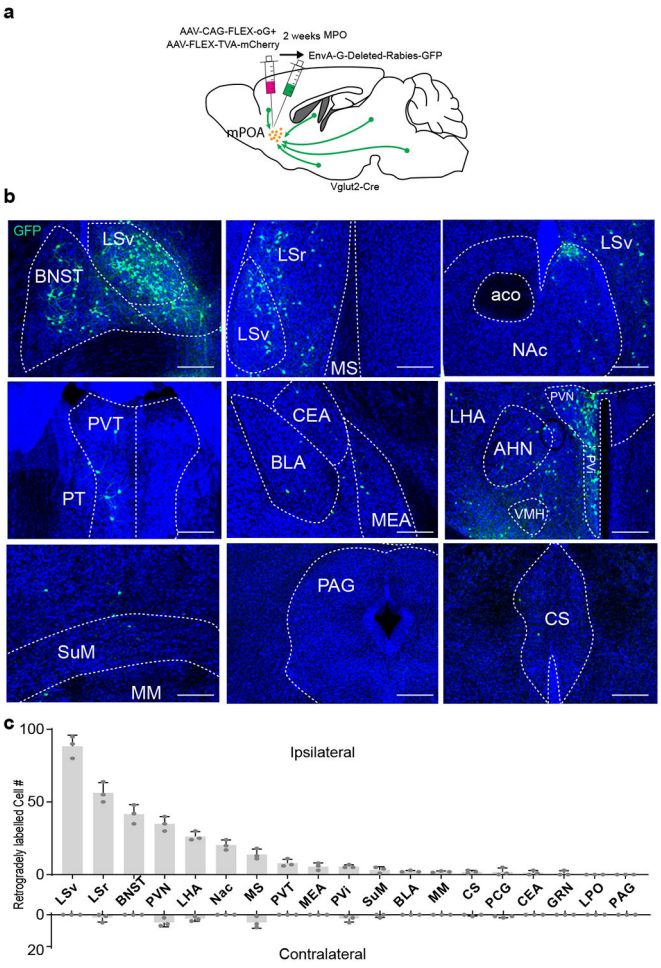

Fig. 7l. Monosynaptic inputs to mPOA glutamatergic neurons.

a, Strategy for cell-type specific tracing of monosynaptic inputs using pseudotyped rabies. **b**, Example images of retrogradely labeled neurons in different brain regions. Scale bar: 500 μm. LSv, lateral septum ventral; LSr, rostral lateral septum; BST, bed nucleus of the stria terminalis; MS, medial septum; NAc, nucleus accumbens; aco, anterior commissure; PVT, periventricular nucleus of the thalamus; PT, parataenial nucleus; BLA, basolateral amygdala; CEA, central amygdala; MEA, medial amygdala; AHN, anterior hypothalamic nucleus; VMH, ventromedial hypothalamic nucleus; PVN, paraventricular hypothalamic nucleus; PVi, periventricular hypothalamic nucleus; SuM, supramammillary nucleus; MM, mammillary nucleus; CS, superior central nucleus raphe. **c**, Quantification of numbers of retrogradely labeled cells in different regions in contralateral and ipsilateral sides of the injected mPOA (n = 3 animals; bar = s.d.). PCG, pontine central gray; GRN, gigantocellular reticular nucleus; LPO, lateral preoptic area. Images in **b** are representative of n=3 animals.